Linköping Studies in Science and Technology. Dissertations.
No. 1055

Ground Object Recognition using Laser Radar Data

Geometric Fitting, Performance Analysis, and Applications

Christina Grönwall

Department of Electrical Engineering
Linköpings universitet, SE–581 83 Linköping, Sweden
Linköping 2006

Ground Object Recognition using Laser Radar Data – Geometric Fitting, Performance Analysis, and Applications

stina@isy.liu.se
www.control.isy.liu.se
Division of Automatic Control
Department of Electrical Engineering
Linköpings universitet
SE–581 83 Linköping
Sweden

ISBN 91-85643-53-X ISSN 0345-7524

Printed by LiU-Tryck, Linköping, Sweden 2006

To Thomas and Arvid

Abstract

This thesis concerns detection and recognition of ground object using data from laser radar systems. Typical ground objects are vehicles and land mines. For these objects, the orientation and articulation are unknown. The objects are placed in natural or urban areas where the background is unstructured and complex. The performance of laser radar systems is analyzed, to achieve models of the uncertainties in laser radar data.

A ground object recognition method is presented. It handles general, noisy 3D point cloud data. The approach is based on the fact that man-made objects on a large scale can be considered be of rectangular shape or can be decomposed to a set of rectangles. Several approaches to rectangle fitting are presented and evaluated in Monte Carlo simulations. There are error-in-variables present and thus, geometric fitting is used. The objects can have parts that are subject to articulation. A modular least squares method with outlier rejection, that can handle articulated objects, is proposed. This method falls within the iterative closest point framework. Recognition when several similar models are available is discussed.

The recognition method is applied in a query-based multi-sensor system. The system covers the process from sensor data to the user interface, i.e., from low level image processing to high level situation analysis.

In object detection and recognition based on laser radar data, the range value's accuracy is important. A general direct-detection laser radar system applicable for hard-target measurements is modeled. Three time-of-flight estimation algorithms are analyzed; peak detection, constant fraction detection, and matched filter. The statistical distribution of uncertainties in time-of-flight range estimations is determined. The detection performance for various shape conditions and signal-to-noise ratios are analyzed. Those results are used to model the properties of the range estimation error. The detector's performances are compared with the Cramér-Rao lower bound.

The performance of a tool for synthetic generation of scanning laser radar data is evaluated. In the measurement system model, it is possible to add several design parameters, which makes it possible to test an estimation scheme under different types of system design. A parametric method, based on measurement error regression, that estimates an object's size and orientation is described. Validations of both the measurement system model and the measurement error model, with respect to the Cramér-Rao lower bound, are presented.

Acknowledgments

First of all, I would like to thank my supervisors Professor Mille Millnert and Professor Fredrik Gustafsson for their guidance in this work and into the world of research in general. I appreciate their support and inspiration during theses years. I am very grateful for the opportunity to work with you both, thank you once again.

Second, I would like to thank the Swedish Defence Research Agency (FOI) for encouraging me do this work, especially Dr. Ove Steinvall, head of the Laser Systems department. No matter how tight his schedule is, he always has time to discuss present and future laser radar systems, both regarding sensors and signal processing. I would also like to thank the previous head of the Sensor Division, Professor Svante Ödman, and the current, Dr. Lena Klasén, for letting me do this work and supporting me financially so that it became possible.

Most of the work have been performed in projects at FOI run by Per Brämming, Leif Carlsson, Tomas Chevalier, Professor Erland Jungert, Svante Karlsson, Dr. Dietmar Letalick, and Stefan Sjökvist. I am very grateful to you and to the other members in the projects. The discussions with Dr. Jörgen Ahlberg, Pierre Andersson, Tomas Chevalier, and Dr. Jörgen Karlholm, among others, have been a great source of inspiration. The data sets used in this thesis have been measured, and preprocessed by TopEye AB, Pierre Andersson, Tomas Chevalier, and Håkan Larsson. Pierre Andersson wrote the first version of the projection code used in papers A,B and E. I thank you all.

I would also like to thank Professor Lennart Ljung and the Automatic Control group, Linköpings universitet, for letting me join the group. Several of you have over the years helped me to sort out the theory, and we had inspiring discussions on signal processing and estimation, especially Dr. Rickard Karlsson and Dr. Jonas Elbornsson. I would like to acknowledge Dr. Johan Löfberg for support with YALMIP, Gustaf Hendeby for the support with LaTeX, and Ulla Salaneck for taking care of all practical matters.

This thesis would not have been written if I had not have such great co-authors of the papers: Dr. Jörgen Ahlberg, Tomas Chevalier, Martin Folkesson, Professor Fredrik Gustafsson, Tobias Horney, Professor Erland Jungert, Dr. Lena Klasén, Professor Mille Millnert, Dr. Ove Steinvall, and Morgan Ulvklo. I have enjoyed all the discussions with you.

I would also like to thank the following colleagues at FOI and the Automatic Control group for proof-reading various parts of the thesis and for all valuable comments and suggestions: Dr. Jörgen Ahlberg, Daniel Ankelhed, Janne Harju, Dr. Rickard Karlsson, Dr. Dietmar Letalick, Per-Johan Nordlund, Dr. Thomas Schön, and Dr. Ove Steinvall.

I appreciate the Grönwall and Carlsson families' encouragement and practical support over the years, especially my mother. Finally, I would like to thank my husband Thomas and our son Arvid for their love, support and patience. This thesis is dedicated to you.

Linköping, October 2006
Christina Grönwall

Contents

Part I

Overview

1

Introduction

In this thesis, detection and recognition of ground objects using laser radar data and performance of laser radar systems are discussed. The focus has been on detection and recognition of vehicles and land mines in outdoor scenes. The objects of interest can be hard to detect by eye, and automatic methods can support the operator. The methods will work in situations where the scene is complex, the objects may be partly hidden or camouflaged and there may be a limited time to perform measurements. For measurement systems and algorithms operating under these conditions, their performance must be analyzed. In this thesis, this is accomplished by modeling the scene and the measurement system.

An example of a scene with land mines and other explosive devices is shown in Figure 1.1. There are wooden sticks, plants and stones in the background that are of similar shape and size as the searched objects.

In Section 1.1, an overview of the topics discussed in this thesis is given and in Section 1.2 the problem is defined. In Section 1.3, an outline of the thesis is given. The main contributions are summarized in Section 1.4.

1.1 Topics

This thesis concerns some types of *man-made objects*. The objects of interest, vehicles and land mines, are also called *targets*, whereas other (uninteresting) objects in the scene are called *clutter*. The objects and the clutter are embedded in a *background*. Usually, the background is the ground level and all objects that are placed on the ground are regarded as objects or clutter. The objects, the clutter, and the background build up the *scene*. In this case, the obtained laser radar data are noisy and the background is unstructured. The noise in data originate from noise in transmitter and receiver, atmospheric phenomena as turbulence and attenuation, and the laser beam's interaction with the object.

In this section, the main problems discussed in the thesis are described, with refer-

Figure 1.1: *In this scene there are 12 explosive devices, a trip wire, and a munition box. From a field test performed by the Swedish Defence Research Agency (FOI).*

ences to the attached papers.

1.1.1 Object Detection and Recognition

The definitions of detection and recognition vary between the application fields. In this thesis, *detection* is defined as the process of distinguishing interesting objects from clutter and the background. The object class determination, i.e., separation of buildings and vehicles, is called *classification*. In the *recognition* process, the object's subclass is determined. For example, a vehicle can be recognized as a car or a truck. Also, the determination of the object's model/make can be included in the recognition process. The automated process for object recognition is called Automatic Target Recognition (ATR) in military applications.

Laser radars can produce high resolution data, where object details can be resolved even at kilometer distances. This can be used for object detection and recognition. Laser radar systems usually produce both 3D and intensity data describing the scene. If this information is combined, robust object detection is possible. There are references where detection is performed on range data and intensity data in parallel, and fused afterward. A first attempt to land mine detection on combined range and intensity data is presented in Paper F.

For recognition of complex objects, like vehicles or buildings, the level of detail makes it possible to identify the major parts of an object. Those main parts, called *functional parts*, can be a factory's chimney, the driver's compartment of a truck, a vehicle's door,

or the barrel of a battle tank. These parts can sometimes vary their orientation relative to the main part of the object, this is called *articulation*. If the functional parts are identified or a building of complex shape can be decomposed into pieces that are easier to process, the recognition task can be simplified. The last step in the recognition process is to match the object data with models from a library, this is called *model matching*. If the object's functional parts are identified, there is an indication of the object type or identity besides the model matching. When performing matching, the list of possible models can thus be reduced. Furthermore, if the object's articulated parts can be identified, the recognition is simplified as the number of degrees of freedom is reduced.

In Paper A, a ground object recognition method based on general, scattered 3D laser radar data is proposed. It is based on the fact that man-made objects of complex shape can be decomposed into a set of rectangles. The method consists of four steps;

1. Estimation of the object's 3D size and orientation,
2. Segmentation of the object into parts of approximately rectangular shape,
3. Identification of segments that contain the functional (main) parts of the object,
4. Matching the object with library models.

The distance between the object and the model is minimized in Least Squares (LS) sense. Functional parts that are subject to articulation are taken into account in the matching. In Paper B a sequential matching is proposed, where the number of functional parts increases in each iteration. The division into parts increases the probability for correct matching, when several similar models are available.

From a computer vision perspective, this sequential processing of data is not optimal. An advantage is the reduction in number of orientations and articulations that need to be tested for each object-model combination and the number of models that are relevant for matching. Further, if a matching model cannot be found, the estimated size and orientation and possibly some identified features can be reported.

Vehicle detection and recognition is a common problem in military applications. There are also applications in safety or security, for example, traffic monitoring and traffic safety. Furthermore, when laser radar is used for mapping of urban areas it can be necessary to detect the vehicles and remove them from the data set, in order to achieve correct maps. There are enormous amounts of mines and unexploded ordinances around the world, that are left in and on the ground after civil wars and international conflicts. With a 3D imaging laser radar the surface-laid devices can be detected. A research goal is to perform the detection in real-time or near real-time. Both international operations and human demining will benefit from fast systems.

1.1.2 Performance Analysis

In object reconstruction and recognition based on laser radar data, knowledge of the range value's accuracy is important. A general 3D imaging laser radar system applicable for hard-target measurements is modeled in Paper C. The statistical distribution of uncertainties in time-of-flight range estimations is determined for three common estimation algorithms; peak detection, constant fraction detection, and matched filter. The detection

performance for various object shape conditions and signal-to-noise ratios is analyzed. The object range is calculated from the time-of-flight estimation, and properties of the uncertainty in range estimation are analyzed. Two simple shape reconstruction examples are shown, and the performance is compared with the Cramér-Rao lower bound.

In Paper D, the performance of a tool for synthetic generation of scanning laser radar data is evaluated. In the tool it is possible to add several design parameters, which makes it possible to test an estimation scheme under different types of system design. The measurement system model includes laser characteristics, object geometry, reflection, speckles, atmospheric attenuation, turbulence, and a direct-detection receiver. A parametric method, based on measurement error regression, that estimates an object's size and orientation is described. Validations of both the measurement error model and the measurement system model are shown.

1.1.3 Applications

The object recognition method presented in Paper A is in Paper E applied in a multi-sensor system for ground object recognition. The system is based on a query language and a query processor, and includes object detection, object recognition, data fusion, presentation and situation analysis. The object recognition is executed in sensor nodes, each containing a sensor and the corresponding signal/image processing algorithms. New sensors and algorithms are easily added to the system. The processing of sensor data is performed in two steps; attribute estimation and matching. First, several attributes, like orientation and dimensions, are estimated from the (unknown but detected) objects. These estimates are used to select the models of interest in a matching step, where the object is matched with a number of object models. Several methods and sensor data types are used in both steps, and data are fused after each step. Experiments have been performed using sensor data from laser radar, thermal and visual cameras.

The object recognition method has also been used for scene analysis, which is presented in Section 3.5. In this application, the contents in two outdoor scenes are analyzed using data from an airborne laser radar. Methods for ground and tree estimation, building reconstruction, and vehicle recognition are combined, to detect and recognize the large objects in the scene.

1.2 Problem Description

Laser radar systems usually return both 3D data and intensity data. In this thesis, the goal has been to develop detection and recognition methods that use the full potential of this data. The measurement situation cannot be controlled, and the detection and recognition methods must handle arbitrary views of the objects. There are different measurement principles and the sampling schemes and the noise properties differ among them. The detection and recognition algorithms must therefore be able to handle data with different properties. The laser radar system and its interaction with the objects in the scene and the atmosphere is quite complicated. To be able to analyze performance of data and algorithms, the generation of laser radar data is modeled. To clarify the system properties, the modeling and performance analysis is presented in a signal processing framework.

The statistical properties of range estimation errors are analyzed. The performance is discussed in terms of the Cramér-Rao lower bound, which is computed analytically or numerically and compared to the actual performance from simulations.

1.3 Outline

Part I contains an overview of laser radar systems, object detection and recognition approaches and approaches for performance analysis of laser radar imaging systems. Parts of the material have been presented earlier in [11, 12, 27, 29, 52, 74, 76, 81]. Part II consists of a collection of papers.

1.3.1 Outline Part I

In Chapter 2, the different types of 3D imaging laser radar systems are described. Properties of laser radar data are described. Methods for detection and recognition of ground objects are presented in Chapter 3. The basis for the recognition method is rectangle fitting, this method is presented first. Work on ground object detection, recognition of articulated objects, and matching of articulated objects with face models is overviewed. A scene analysis application, where the recognition method is used, is presented. Finally, other's work on vehicle detection, vehicle recognition, and detection and recognition of other objects are surveyed. In Chapter 4, the work on performance analysis is overviewed, together with a survey of related work. The models of laser radar systems used in this thesis are presented. Performance bounds on range and intensity data are presented. The thesis is summarized on Chapter 5.

1.3.2 Outline Part II

The work on object recognition is presented in Papers A- B and the work on object detection is presented in Paper F. The analysis of laser radar system performance is presented in Papers C- D. In Paper E, the object recognition method is applied in a query-based multi-sensor system.

Paper A: Ground Target Recognition using Rectangle Estimation

A ground object detection method based on 3D laser radar data is presented. The method handles irregularly sampled 3D data. It is based on the fact that man-made objects of complex shape can be decomposed to a set of rectangles. The method consists of four steps; 3D size and orientation estimation, object segmentation into parts of approximately rectangular shape, identification of segments that represent the object's functional/main parts and object matching with CAD models. The method is tested on vehicle data, collected with four fundamentally different laser radar systems.

Edited version of the paper:

> C. Grönwall, F. Gustafsson, and M. Millnert. Ground target recognition using rectangle estimation. *Accepted for publication in IEEE Transactions on Image Processing*, 2006.

Part of the paper in[1]:

> C. Carlsson and M. Millnert. Vehicle size and orientation estimation using geometric fitting. In *Proceedings SPIE*, volume 4379, pages 412–423, Orlando, April 2001.
>
> C. Carlsson. Vehicle size and orientation estimation using geometric fitting. Technical Report Licentiate Thesis no. 840, Department of Electrical Engineering, Linköping University, Linköping, Sweden, June 2000.

Preliminary version is published as Technical Report LiTH-ISY-R-2735, Department of Electrical Engineering, Linköpings Universitet, Linköping, Sweden.

Paper B: 3D Content-Based Model Matching using Geometric Features

An approach to 3D content-based model matching is presented. It utilizes efficient geometric feature extraction and a matching method that takes articulation into account. The geometric features are matched with the model descriptors, to gain fast and early rejection of non-relevant models. A sequential matching is used, where the number of functional parts increases in each iteration. The division into parts increases the possibility for correct matching results when several similar models are available. The approach is exemplified with a vehicle recognition application, where some vehicles have functional parts.

Edited version of the paper:

> C. Grönwall and F. Gustafsson. 3D content-based model matching using geometric features. *Submitted to Pattern Recognition*, 2006.

Part of the paper in:

> C. Grönwall, P. Andersson, and F. Gustafsson. Least squares fitting of articulated objects. In *Workshop on Advanced 3D Image Analysis For Safety and Security, Proceedings of IEEE Conference on Computer Vision and Pattern Recognition*, pages 116–121, San Diego, CA, June 2005.

Preliminary version is published as Technical Report LiTH-ISY-R-2726, Department of Electrical Engineering, Linköpings Universitet, Linköping, Sweden.

Paper C: Influence of Laser Radar Sensor Parameters on Range Measurement and Shape Fitting Uncertainties

A model of a general direct-detecting laser radar system applicable for hard-target measurements is presented. The laser radar cross sections, i.e., the impulse response of the laser beam's interaction with the object, are derived for some simple geometric shapes.

[1] The author changed name from Carlsson to Grönwall in August 2001.

The cross section models are used, in simulations, to find the statistical distribution of uncertainties in time-of-flight estimations. Three time-of-flight estimation algorithms are analyzed; peak detection, constant fraction detection and matched filter. The detection performance for various shape conditions and signal-to-noise ratios is analyzed. Based on these results, the properties of the uncertainties in range estimation are analyzed. The detector's performances are compared with the Cramér-Rao lower bound.

Edited version of the paper:

> C. Grönwall, O. Steinvall, F. Gustafsson, and T. Chevalier. Influence of laser radar sensor parameters on range measurements and shape fitting uncertainties. *Submitted to Optical Engineering*, 2006.

Preliminary version is published as Technical Report LiTH-ISY-R-2745, Department of Electrical Engineering, Linköpings Universitet, Linköping, Sweden.

Paper D: Performance Analysis of Measurement Error Regression in Direct-Detection Laser Radar Imaging

In this paper, a tool for synthetic generation of scanning laser radar data is described and its performance is evaluated. Data are used for analysis of detection and recognition algorithms. It is possible to modify or add several design parameters in the tool, which make it possible to test an estimation scheme under different types of system designs. The measurement system model includes laser characteristics, object geometry, reflection, speckles, atmospheric attenuation, turbulence and a direct-detection receiver. A parametric method that estimates an object's size and orientation is described. Because measurement errors are present, the parameter estimation is based on a measurement error model. The parameter estimation accuracy is limited by the Cramér-Rao lower bound. Validations of both the measurement error model and the measurement system model are shown.

Edited version of the paper:

> C. Grönwall, T. Carlsson, and F. Gustafsson. Performance analysis of measurement error regression in direct-detection laser radar imaging. In *Proceedings IEEE Conference on Acoustics, Speech and Signal Processing*, volume VI, pages 545–548, Hong Kong, April 2003.

Paper E: Ground Target Recognition in a Query-Based Multi-Sensor Information System

A system covering the complete process for automatic ground object recognition, from sensor data to the user interface, i.e., from low-level image processing to high-level situation analysis, is presented. The system is based on a query language and a query processor, and includes object detection, object recognition, data fusion, presentation and situation analysis. This paper focuses on object recognition and its interaction with the query processor. The object recognition is executed in sensor nodes, each containing a sensor and the corresponding signal/image processing algorithms. Promising results are

reported, demonstrating the capabilities of the object recognition algorithms, the advantage of the two-level data fusion and the query-based system.

Edited version of the paper:

> J. Ahlberg, M. Folkesson, C. Grönwall, T. Horney, E. Jungert, L. Klasén, and M. Ulvklo. Ground target recognition in a query-based multi-sensor information system. *To be submitted*, 2006.

Part of the paper in:

> M. Folkesson, C. Grönwall, and E. Jungert. A fusion approach for coarse-to-fine target recognition. In *Proceedings SPIE*, volume 6242, page 62420H, April 2006.
>
> T. Horney, J. Ahlberg, C. Grönwall, M. Folkesson, K. Silvervarg, J. Fransson, L. Klasén, E. Jungert, F. Lantz, and M. Ulvklo. An information system for target recognition. In *Proceedings SPIE*, volume 5434, pages 163–175, April 2004.
>
> E. Jungert, C. Carlsson, and C. Leuhusen. A qualitative matching technique for handling uncertainties in laser radar images. In *Proceedings SPIE*, volume 3371, pages 62–71, September 1998.

Preliminary version is published as Technical Report LiTH-ISY-R-2745, Department of Electrical Engineering, Linköpings Universitet, Linköping, Sweden.

Paper F: Some Approaches to Object/Ground Segmentation and Object Dimension Estimation

A Bayesian approach to object/background segmentation and object data clustering is proposed. The method uses both 3D and intensity data. An example of land mine detection is shown. Several approaches to object dimension and orientation estimation, based on rectangle estimation, are presented. The estimator's parameter estimation accuracy and execution time are compared in Monte Carlo simulations. In all approaches we take into consideration that there are uncertainties in all dimensions in data, i.e., there is an error-in-variables problem.

Edited version of the report:

> C. Grönwall and F. Gustafsson. Approaches to Object/Ground segmentation and object dimension estimation. Technical Report LiTH-ISY-R-2746, Dept. Electrical Engineering, Linköpings Universitet, Linköping, Sweden, 2006.

Papers not included

There are also other publications of related interest that are not included. Parts of their contents are presented in Part I. The publications are:

G. Tolt, P. Andersson, T.R. Chevalier, C.A. Grönwall, H. Larsson, and A. Wiklund. Registration and change detection techniques using 3D laser scanner data from natural environments. In *Proceedings SPIE*, volume 6396, page 63960A, October 2006.

C. Grönwall, T. Chevalier, Å. Persson, M. Elmqvist, S. Ahlberg, L. Klasén, and P. Andersson. Methods for recognition of natural and man-made objects using laser radar data. In *Proceedings SPIE*, volume 5412, pages 310–320, April 2004.

D. Letalick, J. Ahlberg, P. Andersson, T. Chevalier, C. Grönwall, H. Larsson, Å. Persson, and L. Klasén. 3-D imaging by laser radar and applications in preventing and combating crime and terrorism. In *NATO RTO SCI Symposium on Systems, Concepts and Integration (SCI) Methods and Technologies for Defence Against Terrorism*, volume RTO-MP-SCI-158, London, UK, October 2004.

O. Steinvall, L. Klasen, C. Grönwall, U. Söderman, S. Ahlberg, M. Elmqvist, H. Larsson, and D. Letalick. High resolution three dimensional laser imaging - new capabilities for the net centric warfare. In *Proceedings CIMI (Civil och Militär Beredskap)*, Stockholm, Sweden, May 2003.

O. Steinvall, H. Olsson, G. Bolander, C. Carlsson, and D. Letalick. Gated viewing for target detection and target recognition. In *Proceedings SPIE*, volume 3707, pages 432–448, May 1999.

C. Carlsson, E. Jungert, C. Leuhusen, D. Letalick, and O. Steinvall. Target detection using data from a terrain profiling laser radar. In *Proceedings of the 3rd International Airborne Remote Sensing Conference and Exhibition*, pages I–431 – I–438, Copenhagen, Denmark, July 1997.

C. Carlsson, E. Jungert, C. Leuhusen, D. Letalick, and O. Steinvall. A comparative study between two target detection methods applied to ladar data. In *Proceedings of the 9th Conference on Coherent Laser Radar*, pages 220–223, Linköping, Sweden, June 1997.

1.4 Contributions

The main contributions in the thesis are:

Paper A: An approach to ground object recognition that can handle general, irregularly sampled 3D data and arbitrary perspective of the object. Articulated parts of the object are identified. The approach is tested on data from field experiments from four fundamentally different systems operating in different aspect angles.

Paper B: An iterative, least squares matching of 3D point scatter and face models that includes outlier rejection is proposed. The matching method is modular and the object's articulated parts are connected to the main part in a controlled way. A penalty function for selection of the number of functional parts is also proposed.

Paper C: The laser radar system is described in a channel model context, which clarifies the system's properties from a signal processing view. It is shown by simulations that the range error can be modeled as Gaussian distributed, with bias and variance that are functions of object shape and signal-to-noise ratio.

Paper D: The Cramér-Rao lower bound for line estimation under the presence of measurement errors is derived. It is shown in simulations that both the laser radar model and the measurement error model are close to the Cramér-Rao lower bound.

Paper E: A query-based system for ground object recognition based on multi-sensor data is demonstrated. It is shown in an example how the two-level fusion and the division of the object recognition into two steps improve performance and decrease computational complexity. The author's contributions are the attribute estimation and model matching methods for 3D data, co-development of the computational model and being the first author of the paper.

Paper F: An approach to Bayesian object/background segmentation and object clustering is presented. Both 3D and intensity data are used in the approach. Several formulations of the rectangle fitting problem are presented and compared with respect to parameter estimation accuracy and execution time.

2

Laser Radar Systems

Laser radar systems have been investigated over several decades primarily for military applications, see for instance [43]. Laser radars are, just as conventional radars (radio detection and ranging), mainly used for remote sensing. Laser radar is sometimes called *ladar* (laser detection and ranging or laser radar) or *lidar* (light detection and ranging). As in microwave radar technology, the range to object and background is often obtained by measuring the time-of-flight for a modulated laser beam from the transmitter to the object and back to the receiver. Some unique features in laser radar systems are high angular, range and velocity resolution.

Two main detection schemes can be identified in laser radar systems; coherent and direct-detection. In coherent detection, the phase information is preserved. The returning signal is mixed with a local oscillator and the signal at the difference frequency is detected. These types of systems is common for aerosol measurements, and velocity and vibration measurements with very high accuracy.

In direct-detection systems, the phase information is lost as the returning signal is simply collected on a detector. Direct-detection laser radar systems are less complex and are common in 3D imaging applications. There are several principles for direct-detection 3D imaging laser radar; scanning, staring and gated viewing. The main measurement principles are described in Section 2.1. This section is based on the laser radar descriptions in [52, 74]. In Section 2.2, the data types from those systems are discussed.

2.1 Measurement Techniques

The first laser radar systems were *single point sensors* and in the 1980's the single point sensors were combined with rotating mirrors to achieve *scanning systems*. This was the first type of 3D imaging laser radar.

A straight-forward method to acquire 3D information of a scene is to scan the object with a single point detector laser radar. With every laser pulse, a very small part of the object is illuminated and the time-of-flight of the reflected pulse is stored. Some detectors give a time-resolved pulse response (full waveform), whereas other detectors only give the time for the pulse return (above a certain threshold). With some systems it is possible to store first and last echo, or even more returns, each echo representing a different object range. There are also line array scanners, where an array of point sensors are used. An advantage of a scanning system is the possibility to achieve high angular resolution. The main disadvantage is the long data acquisition time, which prevents the capture of moving objects.

The development of Focal Plane Array (FPA) detectors with timing capability in each pixel has made non-scanning 3D imaging laser radars feasible [78, 79]. These *staring systems* (flash laser radars) enable the capture of a complete 3D image with just one transmitted laser pulse. With such a system, the frame rate can be increased to video rate (50 Hz or 60 Hz), data from moving objects can be obtained. The sensor has the same size as an ordinary camera, excluding the laser source, which can be fit to the application, and the data acquisition platform, normally a computer. In short range systems, the laser can be incorporated into the camera unit itself.

With the *Gated Viewing* (GV) technique, also called burst illumination, the sensor can be a simple camera constructed for the laser wavelength, but the shutter gain is synchronized with an illuminating short pulse laser [76]. This enables image collection at certain range interval in the scene. With an adjustable delay setting, corresponding to the time-of-flight back and forth to a desired range, the opening of the camera shutter is controlled. This exposes the camera only for a desired range slice, with the slice as deep as the shutter open time. The delay can be changed through a predefined program, resulting in a number of slices representing different ranges, i.e., a 3D volume. The set-back of this system is the power inefficiency, since every range slice image requires a total scene illumination. The advantage is the low cost and robustness, since rather simple components can be used. It has been shown that a rather small set of gated images can give high resolution 3D images, if the depth information is taken into account [4, 52]. The process is illustrated in Figures 2.1- 2.2.

From a signal processing point of view, the benefits and drawbacks with laser radar measurements can be summarized as:

- A laser radar system returns range and intensity data with high angular precision. This data are, however, noisy and there are sometimes artifacts at borders of objects. This is a type of aliasing phenomenon, resulting in object samples that are placed behind and above the object. The returned intensity values in the image are a function of the object's surface properties, which can be used to distinguish different materials. On the other hand, the returned intensity is a function of all objects that the laser beam has enlightened. This means that for partly obscured objects, the returned intensity for an object can vary severely over the surface.

- The active illumination with a laser results in complete independence of ambient light conditions (such as day or night), and hence the image contrast is very robust in that respect. On the other hand, the illumination can be detected.

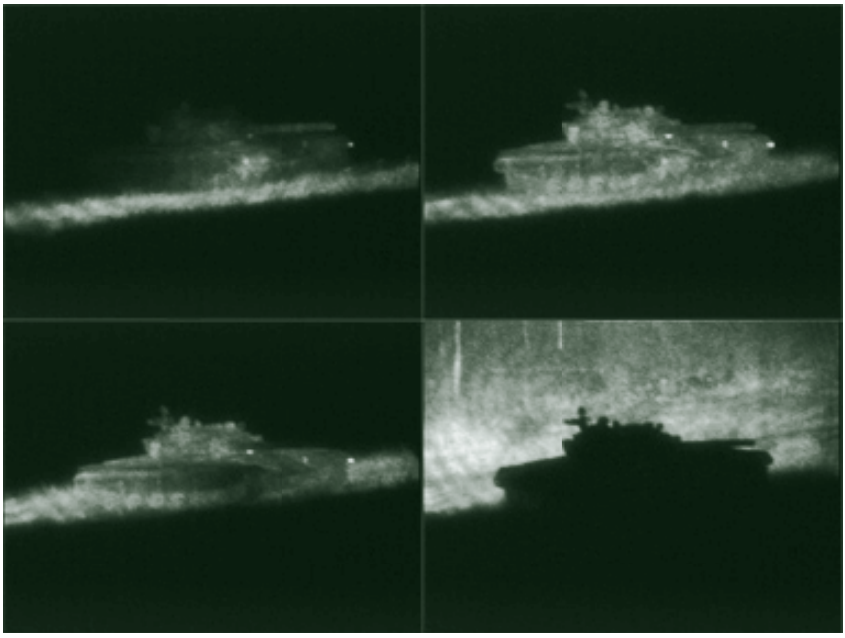

Figure 2.1: *A sequence of GV images collected at four distances. This results in laser reflections from the foreground, object's front, entire object and background. From [52].*

Figure 2.2: *Two views of an object reconstructed from a sequence of GV measurements. From [52].*

- The short wavelength makes it possible to collect data of high resolution. Details of the object can be acquired, which is powerful in recognition applications. On the other hand, when large objects or scenes are measured a lot of data are collected. This requires fast hardware, large storage capabilities and fast algorithms.
- Due to the short wavelength, laser radars are more sensitive than conventional radars to atmospheric conditions with high attenuation, like fog, but less sensitive to rain and snow. This drawback can be partly compensated by the gating technique [76].
- The laser beam has a small footprint, resulting in that sparse structures can be penetrated. This adds the ability to collect data from objects that are partly hidden behind vegetation, camouflage nets, curtains, or Venetian blinds.
- The laser radar does not penetrate dense structures, as tree stems, metal surfaces, roofs, and walls. Those object types do not transmit the particular wavelength. This means that data are only collected from the parts of the objects that are in the line of sight from the sensor. This effect is called *self-occlusion* and a *2.5D* representation of the scene is collected.

2.2 Laser Radar Data

With 3D laser radar a new dimension is added to active imaging. In addition to intensity and angular coordinates, also range is included in the image. A scanning or staring laser radar usually gives both an intensity and a range image of the scene. When an object is measured with these types of a laser radars, a 3D coordinate is retrieved in each sample. This means that data can be projected to an arbitrary view. In Figure 2.3, the data formats are shown. It is only a 2.5D presentation of the scene, due to the self-occlusion. To achieve a full 3D representation of the scene, 2.5D images collected from various positions are combined. That process is called *registration* and an approach for registration in forested scenes is presented in [81]. Registration is not within the scope of this thesis.

In this work, focus is on unstructured point scatter data that give a 2.5D representation of the object. The data sets come from both scanning and GV systems. Processing of unstructured point data gives the opportunity to work with high-resolution data, the drawback is the long processing time for large data sets. Large data sets are common in the detection phase, where interesting objects are identified. In that phase, the processing time can be decreased if traditional image processing techniques are applied to the intensity and range images. Once the interesting parts in the scene are identified, the point scatter data can be used to achieve detailed detection and recognition with higher accuracy.

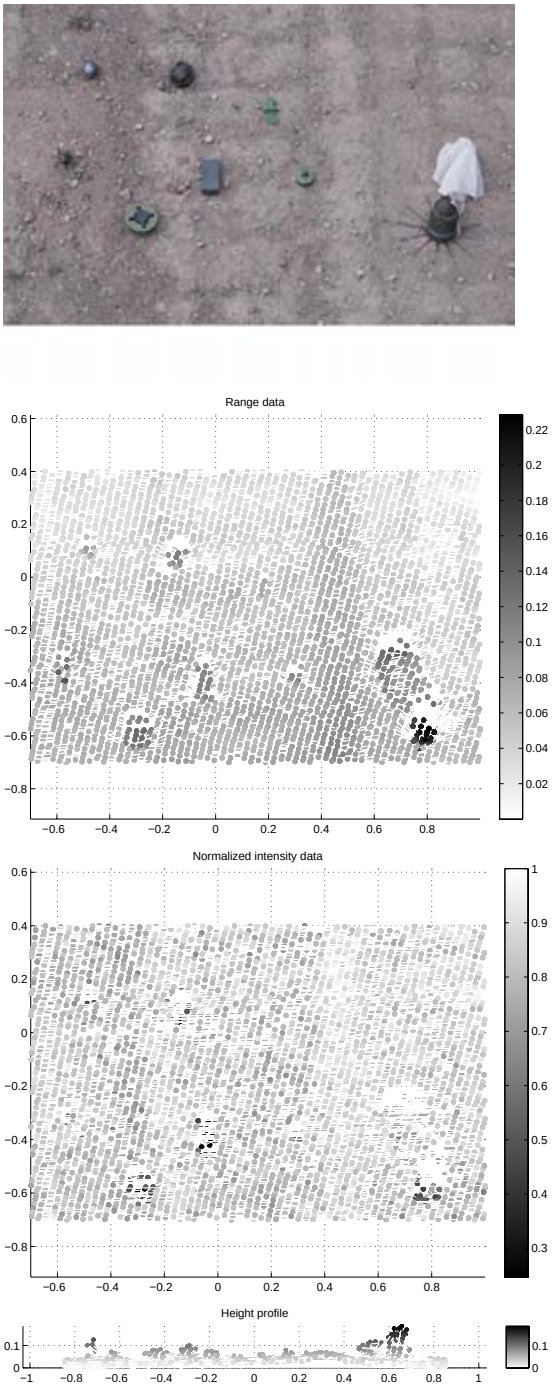

Figure 2.3: *A gravel road with mines. From top to bottom: photograph, range data, normalized intensity data, and range data projected to height profile. Axes in meters.*

3

Ground Object Detection and Recognition

The amount of research in detection and recognition is vast, even when it is constrained to applications where laser radar data are used, or to a certain object type. In the application types considered here, the scene cannot be controlled during the measurement. The object's orientation relative to the sensor and the orientation of articulated parts, if they exist, are arbitrary. The ground level is not assumed to be known, which means that the object/ground segmentation problem must be solved. The background is unstructured. There is also self-occlusion and there may be other objects that partly occlude the object.

The core of the object recognition process is rectangle fitting. The method used in this work in presented in Section 3.1. There has been work reported on mine detection using metal detectors together with ground penetrating radars [16], visual sensors [15], InfraRed (IR) sensors [9, 35, 37, 54, 58] and laser vibrometry [64]. To the author's knowledge, 3D and intensity laser radar data have not been used for mine detection. Initial work on mine detection using 3D and intensity laser radar data is reported in Paper F. This work is shortly described in Section 3.2. The work on recognition of articulated objects and model matching is overviewed in Sections 3.3- 3.4. In Section 3.5, an approach to scene analysis is presented. It has been presented earlier in [29] and the object recognition approach presented in Paper A is applied. There are many applications of vehicle detection and recognition methods using laser radar data reported. These are surveyed in Sections 3.6- 3.7. In Section 3.8, object detection and recognition applications in other areas are presented.

3.1 Rectangle fitting

The basis for the object recognition approach presented in the thesis is rectangle fitting. The method has been described separately as *Rotating Calipers* [83] and in [10, 13]. A short description of the method is presented in this section, evaluation of its performance

is found in Paper A, Paper F, and [33].

A straight line in 2D can be described as $n_1 x + n_2 y - c = 0$, where $\varphi_i = (x_i, y_i)$ contains data, the normal vector $\mathbf{n} = (n_1, n_2)^t$ defines the slope of the line, c is the distance to origin, and x^t is matrix transpose. The object points $\varphi_i, i = 1, ..., N$ are inside or on the side of the rectangle if

$$\text{Side 1} : n_1 x_i + n_2 y_i - c_1 \geq 0, \quad i = 1, ..., N \tag{3.1a}$$

$$\text{Side 2} : -n_2 x_i + n_1 y_i - c_2 \geq 0, \quad i = 1, ..., N \tag{3.1b}$$

$$\text{Side 3} : n_1 x_i + n_2 y_i - c_3 \leq 0, \quad i = 1, ..., N \tag{3.1c}$$

$$\text{Side 4} : -n_2 x_i + n_1 y_i - c_4 \leq 0, \quad i = 1, ..., N \tag{3.1d}$$

where $\mathbf{n}^t \mathbf{n} = 1$, and X^t is matrix transpose. The normal vector (n_1, n_2) is orthogonal to side 1 and side 3 of the rectangle, the normal vector $(-n_2, n_1)$ is orthogonal to side 2 and side 4 of the rectangle and c_i is the Euclidean distance between side i and the inertia point of the rectangle, $i = 1, 2, 3, 4$. By introduction of the rotation matrix

$$\mathbf{R}^+ = \begin{pmatrix} 0 & -1 \\ 1 & 0 \end{pmatrix},$$

the parameter vector $\theta = (n_1, n_2, c_1, c_2, c_3, c_4)^t$, the regression vector $\varphi = (\varphi_1, ..., \varphi_N)^t$, $\mathbf{1} = (1, 1, ..., 1)^t$ (column with N ones), and $\mathbf{0} = (0, 0, ..., 0)^t$ (column with N zeros), (3.1) can be written as

$$\begin{pmatrix} \varphi & \mathbf{-1} & \mathbf{0} & \mathbf{0} & \mathbf{0} \\ \varphi \mathbf{R}^+ & \mathbf{0} & \mathbf{-1} & \mathbf{0} & \mathbf{0} \\ -\varphi & \mathbf{0} & \mathbf{0} & \mathbf{1} & \mathbf{0} \\ -\varphi \mathbf{R}^+ & \mathbf{0} & \mathbf{0} & \mathbf{0} & \mathbf{1} \end{pmatrix} \theta \geq 0. \tag{3.2}$$

A rectangle that contains all samples φ inside or on the rectangle's edge is found by

$$\min \quad (c_3 - c_1)(c_4 - c_2) \tag{3.3a}$$

subject to

$$\begin{pmatrix} \varphi & \mathbf{-1} & \mathbf{0} & \mathbf{0} & \mathbf{0} \\ \varphi \mathbf{R}^+ & \mathbf{0} & \mathbf{-1} & \mathbf{0} & \mathbf{0} \\ -\varphi & \mathbf{0} & \mathbf{0} & \mathbf{1} & \mathbf{0} \\ -\varphi \mathbf{R}^+ & \mathbf{0} & \mathbf{0} & \mathbf{0} & \mathbf{1} \end{pmatrix} \theta \geq 0 \tag{3.3b}$$

$$\mathbf{n}^t \mathbf{n} = 1. \tag{3.3c}$$

This rectangle will also contain the convex hull of the data set. This problem is not convex, as the objective function and the last constraint are not convex. There is a constraint that limits the number of possible orientations of the rectangle, see Theorem 3.1.

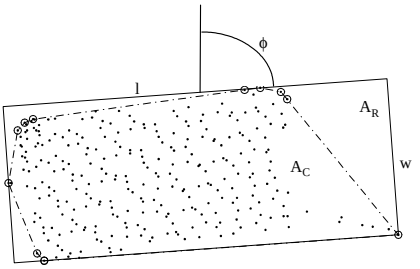

Figure 3.1: *Illustration of the rectangle estimation. A set of samples (dots), the convex hull (dashed line), and the estimated rectangle (solid line) are shown. The samples belonging to the convex hull are encircled. The length (l), width (w), orientation (ϕ), convex hull area (A_C), and rectangle area (A_R) are indicated.*

Theorem 3.1 (Minimal Rectangle)
The rectangle of minimum area enclosing a convex polygon has a side co-linear with one of the edges of the polygon.

Proof: See [22] for the first proof. The proof is also performed in [62] using angle calculations and in [10] using linear algebra. □

Using this theorem, the number of possible orientations of the rectangle are limited, only rectangles that have one side co-linear with one of the edges of the convex hull have to be tested. An example is shown in Figure 3.1. In both [10] and [83] (similar) algorithms are given for calculation of the minimal area in linear time, i.e., $O(N_v)$ where N_v is the number of vertices in the convex polygon. Further, the convex hull can be calculated in $O(N \log_2 N)$ time, where N is the number of samples and $\log_2$ the logarithm function with base 2, if data are unsorted and in $O(N)$ time if data are sorted.

3.2 Object detection

Early work on vehicle detection, based on 3D data, is presented in [11, 12]. That approach can only handle vehicles that are placed on a relatively flat surface in open terrain with clear separation from the background. The rectangle fitting method can also be used for object/background segmentation, this is applied as preprocessing in Papers A- B. The slope of the ground surrounding the object is estimated by projections of 3D data. The 3D data are represented by (x, y, z), where (x, y) is position and (z) is range. First the slope is estimated in (x, z) projection and the data set is rotated so that the background is flat in that projection, we now have the coordinates (x', z'). The slope estimation and rotation is then repeated for the (y, z') projection. The result is a rotated coordinate system (x', y', z''), where (x', y') is position on a flat surface and (z'') are height values. When the ground is flat, the object and ground can be separated by height. An example is shown in Figure 3.2.

These types of detection and object/background segmentation methods apply for the simple case with relative flat ground surface and no occluding clutter or background.

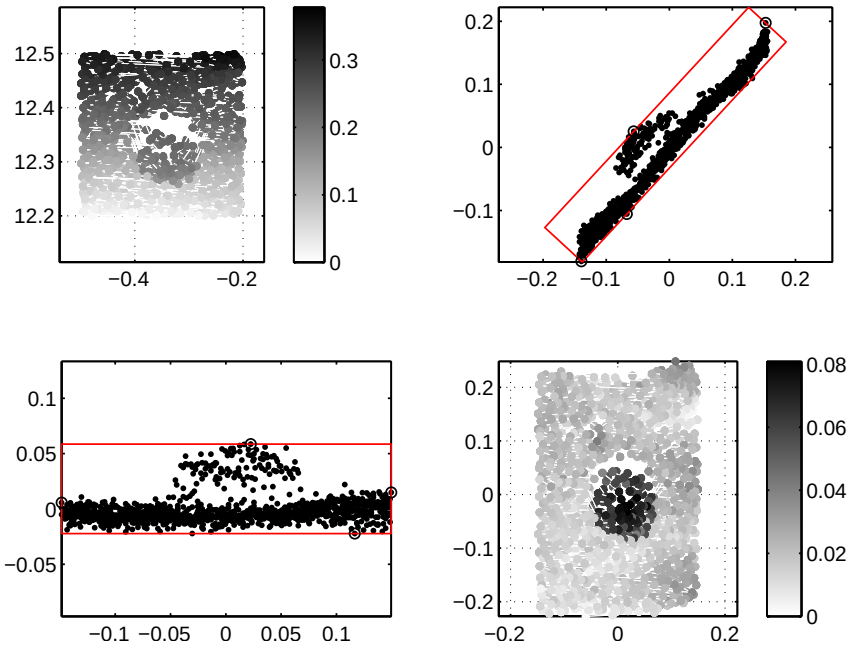

Figure 3.2: *Example of rotation of a scene (land mine on gravel road). Top, left: original range data in (x, y, z) coordinates, top, right: estimated rotation in (x, z) projection, bottom, right: estimated rotation in (y, z') projection, bottom, right: final data set in (x', y', z'') coordinates.*

Figure 3.3: *Photograph of two mines on a gravel road.*

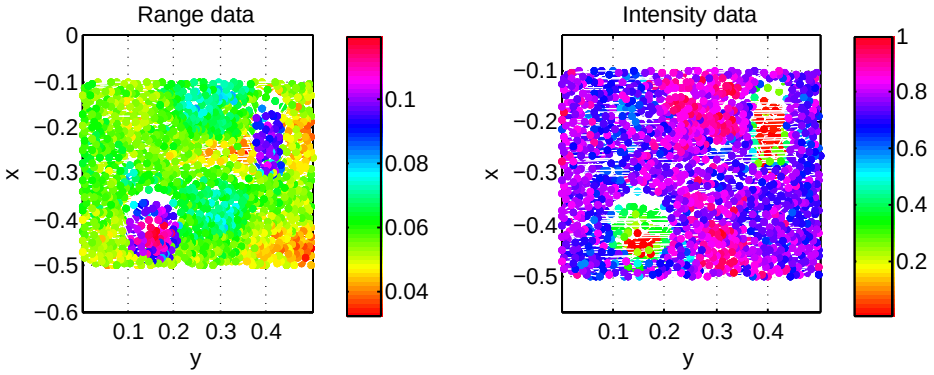

Figure 3.4: *Range data (left) and normalized intensity data (right) of the mine scene, axes in meters.*

Furthermore, these methods do not take advantage of the intensity information in the data set.

In Paper F, a Bayesian approach for object/background segmentation is proposed. For separation of data into object and background samples, and estimation of the variances of the classes, Gaussian mixture based on Expectation Maximization (EM) is used. A mixture of two Gaussian functions is fitted to data. These estimates are used as a priori information in a Bayesian classifier. Bayesian hypothesis testing for two classes is applied for classification of data into object and background data and clustering of object data.

This approach was tested on a scene with two mines on a gravel road, see Figure 3.3 for a photograph of the scene and Figure 3.4 for range and intensity data. The mixture of two Gaussian functions fitted to the combined range and intensity data is shown in the left part of Figure 3.5. In the right part of Figure 3.5, the segmentation and clustering of data are shown. Both objects are detected and clustered with few miss-classifications. This is the first result and further studies are needed. For example, higher order Gaussian mixtures that include position, and more complicated scenes must be investigated. A detailed description is found in Paper F.

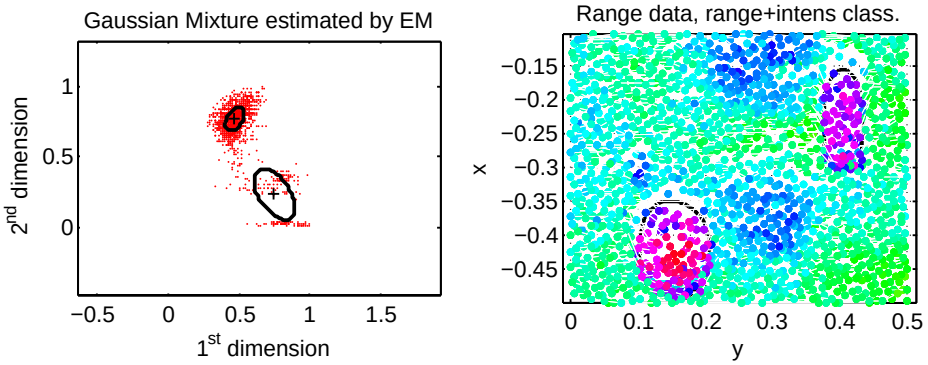

Figure 3.5: *Two-dimensional Gaussian mixture estimation (left) and the resulting classification and clustering (right). Axes in meters in the right part.*

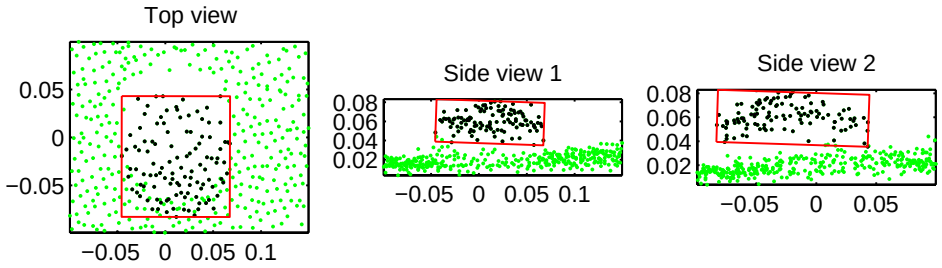

Figure 3.6: *An example of dimension and orientation estimation of the mine in Figure 3.2. Object data (black), background data (gray), and the estimated rectangles are shown. Axes in meters.*

3.3 Recognition of Articulated Objects

In [10, 13], it was shown that the rectangle fitting method could be used for dimension and orientation estimation of man-made objects. An example of rectangle fitting of the mine in Figure 3.2 is shown in Figure 3.6.

The rectangle fitting method has also been used in an approach for recognition of articulated objects, see Paper A. In Paper B, a penalty function for the number of functional parts, and an iterative least squares fitting method with outlier rejection are proposed.

The method handles general, irregularly sampled, scattered, 3D data. It takes advantage of the 3D structure and that the dimensions are known in laser radar data. The estimation of initial position and segmentation into functional parts is based on the assumption that man-made objects, like vehicles and buildings, in certain projections are of rectangular shape. A man-made object of complex shape can be decomposed into a set of rectangles and in some views the rectangles will describe the functional parts of the object. In this application we cannot assume that the object is placed in a certain orientation relative to the sensor or that the object is articulated in a specific way.

The object recognition method consists of four steps:

1. Estimate the object's 3D size and orientation using the rectangle estimation method described in Section 3.1.
2. Segment the object into parts of approximately rectangular shape. The functional parts can be found in some of the rectangles.
3. Identify the functional parts by simple geometric comparisons and estimate their dimensions and orientations.
4. Match the entire object with a wire-frame model. The model's functional parts are rotated to the estimated orientations.

The goal with identification and fitting of functional parts for vehicles is to simplify the model matching. If the object's parts are identified, matching with model can be performed regardless of the relative position of the functional parts. Different configurations of a vehicle can be handled in a structural way. If the functional parts of a tank (the barrel and turret) can be extracted, the hypothesis that the object is a tank is strengthened. When the object's functional parts are identified, the recognition can be simplified as the number of degrees of freedom reduce. Further, for a tank the orientation of the barrel indicates the tank's intention, which can be useful in security or military applications.

An example of identification of functional parts for a tank is shown in Figure 3.7. The segmentation into rectangular parts are performed in top, side, and front/back view projections. For every projection the segmentation is performed along both the main and the secondary axis, where the axis are estimated with rectangle fitting. In total, the object is segmented in six different ways and all rectangles are compared with the library model's main parts using geometric rules for dimensions and orientations. The matching with a face model (CAD model) is shown in Figure 3.8.

3.4 Matching of Articulated Objects with Face Models

The model matching in Paper A is based on global matching of data and model. This approach can be developed to modular matching, where the articulated parts are matched in controlled way. Further, to control the number of articulated parts that are valid for the particular data set, a penalty function is proposed. This work is presented in Paper B and [27]. First, LS fitting with point correspondence between the data set and the model is described. After that, the case where point correspondence is not present is described. In the latter case it is common to use the Iterative Closest Point (ICP) [8]. An extension of ICP that includes outlier rejection is proposed.

3.4.1 LS Fitting with Point Correspondence

First, the global LS fitting problem of two 3D point scatters with point correspondences is presented [7]. The problem is then extended to modular LS fitting where the object's articulation is treated, as proposed in [27] and Paper B.

Assume that there are two 3D point sets $P = (p_1, p_2, ..., p_N)^t$ ($N \times 3$) and $Q = (q_1, q_2, ..., q_N)^t$ ($N \times 3$) that are related by $Q = (P\mathbf{R} + \mathbf{T}) + E$, where $\mathbf{R}$ is a

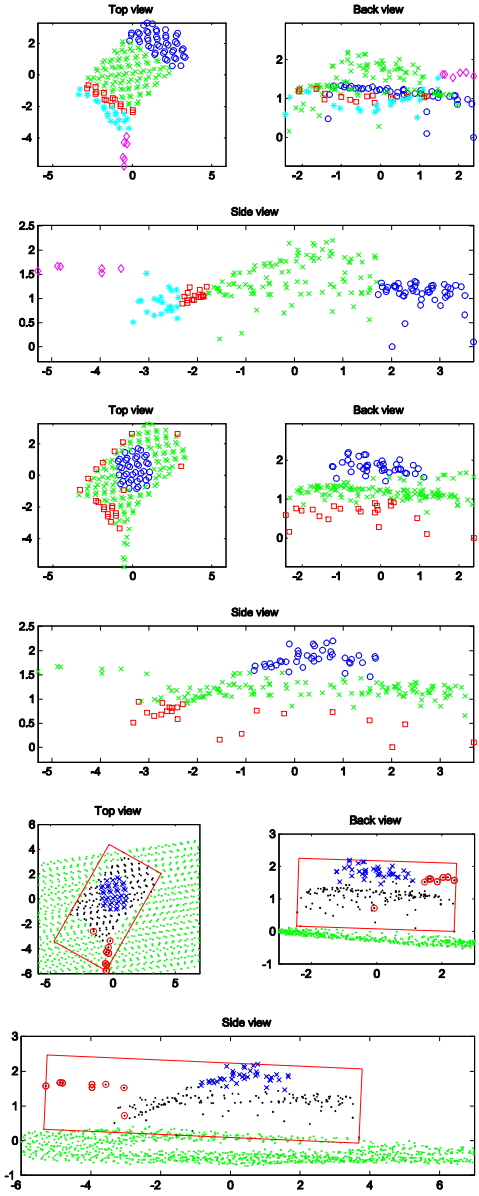

Figure 3.7: *Result of size and orientation estimation, segmentation and node classification. Top: side view, short side segmentation. Data are divided into five segments, where one is identified as a barrel (marked with rhombus). Middle: side view, long side segmentation. Data are divided into three segments, where one is identified as a turret (marked with circles). Bottom: the rectangles show the estimated size and orientation. Identified barrel samples are marked with 'o' and turret samples with 'x'. Axes in meters.*

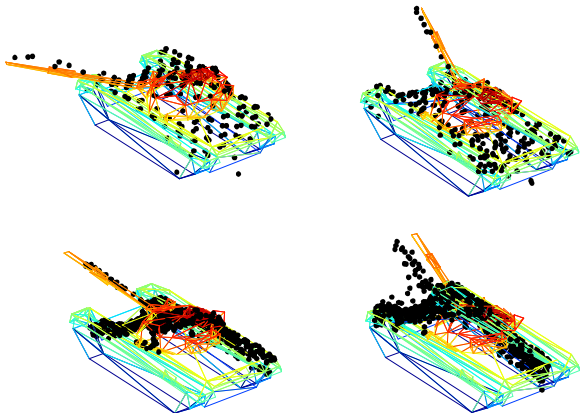

Figure 3.8: *Matching results, tank (T72) data collected with three different laser radar systems are matched with the T72 model.*

rotation matrix, $\mathbf{T}$ is a translation vector and $E = (e_1, e_2, ..., e_N)^t$ is noise. The (noise free) model is represented by Q and the noisy object by P. The noise $e_i, i = 1, ...N$, has zero mean, equal variance and the elements in E are independently and identically distributed (i.i.d.). In the global LS method, the goal is to find $\mathbf{R}$ and $\mathbf{T}$ that in least squares sense minimize

$$V = \min_{\mathbf{R},\mathbf{T}} \quad \|Q - (P\mathbf{R} + \mathbf{T})\|_2^2 \tag{3.4a}$$

$$\text{subject to} \quad \mathbf{R}\mathbf{R}^t = \mathbf{I} \tag{3.4b}$$

$$\det \mathbf{R} = 1, \tag{3.4c}$$

where V is the Mean Square Error (MSE), $\|\cdot\|_2$ is the Euclidean norm, and $\mathbf{I}$ is the identity matrix. Define the regressor ϕ and the parameter vector θ

$$\varphi^t = \begin{pmatrix} P & \mathbf{1}_{N\times 1} \end{pmatrix}$$
$$\theta = \begin{pmatrix} \mathbf{R}^t & \mathbf{T} \end{pmatrix}^t,$$

where $\mathbf{1}_{N\times 1} = (1, 1, ..., 1)^t$. The minimization problem (3.4) can then be written

$$V = \min_{\theta} \quad \left\|Q - \varphi^t\theta\right\|_2^2 \tag{3.5a}$$

$$\text{subject to} \quad \mathbf{R}\mathbf{R}^t = \mathbf{I} \tag{3.5b}$$

$$\det \mathbf{R} = 1. \tag{3.5c}$$

Assume that the functional parts of the object are identified, that the data set can be divided into these parts, and that it is possible to do the same division with the model. Further, assume that the object has a main part and on that part, another part is placed and on that second part a new part is placed, etc. The general case with model and object data

divided into J parts, can be expressed,

$$\begin{aligned}
Q_1 &= P_1\mathbf{R}_1 + \mathbf{T}_1 + E_1 \\
Q_2 &= (P_2\mathbf{R}_1 + \mathbf{T}_1)\,\mathbf{R}_2 + \mathbf{T}_2 + E_2 \\
&\vdots \\
Q_J &= P_J\mathbf{R}_J + \mathbf{T}_J + E_J \\
\mathbf{R}_J &= \mathbf{R}_1\mathbf{R}_2\cdots\mathbf{R}_{J-2}\mathbf{R}_{J-1} \\
\mathbf{T}_J &= \mathbf{T}_{J-2}\mathbf{R}_{J-1} + \mathbf{T}_{J-1},
\end{aligned}$$

where the elements in $E = \begin{bmatrix} E_1 & E_2 & \cdots & E_J \end{bmatrix}^t$ are i.i.d. with zero mean and equal variance. Part P_j contains N_j samples, $N_1 + N_2 + \cdots + N_J = N$. Define φ^t and θ as

$$\varphi^t = \begin{pmatrix}
P_1 & \mathbf{0} & \mathbf{0} & \mathbf{0} & \mathbf{1} & \mathbf{0} & \cdots & \mathbf{0} \\
\mathbf{0} & P_2 & \mathbf{0} & \mathbf{0} & \mathbf{0} & \mathbf{1} & \cdots & \mathbf{0} \\
\cdots & \cdots & \cdots & \cdots & \cdots & \cdots & \cdots & \cdots \\
\mathbf{0} & \mathbf{0} & \cdots & P_J & \mathbf{0} & \mathbf{0} & \cdots & \mathbf{1}
\end{pmatrix},$$

$$\theta = \begin{pmatrix} \mathbf{R}_1^t & \cdots & \mathbf{R}_J^t & \mathbf{T}_1 & \cdots & \mathbf{T}_J \end{pmatrix}^t,$$

where $\mathbf{1} = (1, 1, ..., 1)^T$ (column with N_j ones), and $\mathbf{0} = (0, 0, ..., 0)^T$ (column with N_j zeros). Then the modular LS fitting problem can be defined as

$$V = \min_{\theta} \quad \left\|Q - \varphi^t\theta\right\|_2^2 \tag{3.6a}$$

$$\text{subject to} \quad \mathbf{R}_j\mathbf{R}_j^t = \mathbf{I}, \quad j = 1, ..., J \tag{3.6b}$$

$$\det \mathbf{R}_j = 1, \quad j = 1, ..., J \tag{3.6c}$$

This formulation makes it possible to control the interrelations between the different parts of the object.

An illustration is shown in Figure 3.9. The vertices of a facet model is used as the point set representing the model and a rotated and translated copy of the model samples represents the object. The object samples are contaminated with Gaussian noise with zero mean and variance of 0.01 m^2 (on an object of approximately 9.65×3.52×2.49 meter). In Figure 3.9, the results of global LS fitting (3.5) and the result of modular LS fitting (3.6) are shown. The MSE is reduced approximately 500 times in this case. The model samples are represented by the facet model in the figure.

3.4.2 LS Fitting of 3D Points and Face Model

In most cases, two point sets with point correspondence are not available. Instead there is a point scatter describing the object and the model is a face model, denoted $\mathcal{M}$. It is then possible to fit the object samples with their projections on the closest facets. Due to the projections, the fitting problem is a nonlinear problem which can be solved within the ICP framework. Define P as the point set describing the object and Q as the point set describing the model, where Q is the projection of the elements in P to the closest model facet, i.e.,

$$P = \text{Proj}\,(Q|\mathcal{M})\,.$$

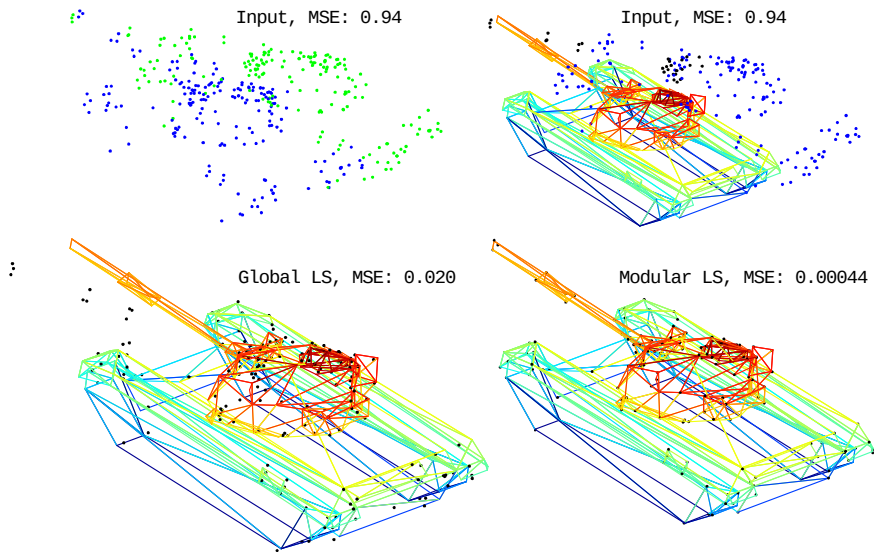

Figure 3.9: *Geometric fitting of two point scatters with point correspondence. The two point scatters (top, left), the model point scatter represented by the face model (top, right). Fitting using global LS (bottom, left) and modular LS (bottom, right). The MSE of the fit is given.*

If the orthogonal projection of an element in P is not on a facet, the projected sample is set to the closest facet edge. First, the ICP algorithm proposed by Besl and McKay [8] is presented, then follows an extension with outlier rejection and modular matching.

The original ICP algorithm was presented in [8], in Algorithm 1 it is rewritten in the notation used in this thesis.

Algorithm 1. Iterative Closest Point

1. For iteration k, calculate the closest points of $P_j^k, j = 1, ..., J$ on the model $\mathcal{M}$, $Q_j^k = \text{Proj}\left(P_j^k | \mathcal{M}\right)$, to get point correspondences.
2. Estimate rotations $\mathbf{R}^k$ and translations $\mathbf{T}^k$.
3. Calculate the MSE of the estimation error, $V^k\left(\mathcal{M}\right)$, see (3.6).
4. If $\tau > V^{k-1}\left(\mathcal{M}\right) - V^k\left(\mathcal{M}\right)$, terminate. Otherwise, continue to iteration $k+1$. The threshold τ is user-defined.

In applications with noisy data an outlier rejection is needed; elements in Q that have too long distances to the corresponding samples in P will be rejected. The outlier distance depends on the uncertainty in data and the resolution in the face model. An iterative algorithm for fitting a 3D point set with a face model, when the number of functional parts is fixed to J, is proposed in Algorithm 2.

Algorithm 2. Modular ICP with Outlier Rejection

1. Estimate the object's orientation, including orientation of functional parts, and place the model in similar position. This gives the initial rotations $\mathbf{R}_1^0, \cdots, \mathbf{R}_J^0$ and translations $\mathbf{T}_1^0, \cdots, \mathbf{T}_J^0$.
2. For iteration k, calculate the closest points of $P_j^k, j = 1, ..., J$ on the model $\mathcal{M}$, $Q_j^k = \text{Proj}\left(P_j^k | \mathcal{M}\right)$, to get point correspondences.
3. Reject outlier elements in Q_j^k and their corresponding elements in $P_j^k, j = 1, ..., J$.
4. Estimate rotations $\mathbf{R}_1^k, \cdots, \mathbf{R}_J^k$, and translations $\mathbf{T}_1^k, \cdots, \mathbf{T}_J^k$, and calculate the MSE of the estimation error, $V^k(\mathcal{M})$, see (3.6).
5. If $\tau < V^k(\mathcal{M}) / V^{k-1}(\mathcal{M})$, terminate. Otherwise, continue to iteration $k+1$. The threshold τ is user-defined.

If Algorithm 2 is compared with Algorithm 1, the outlier rejection in step 3 is added and the termination criterion is relative instead of absolute. The impact of the outlier rejection is illustrated in Figure 3.10. The data set is simulated using the vertex points from a model (a T72 chassis), the samples are rotated 10 degrees and translated 0.5 meter in 3D. Gaussian noise with zero mean and standard deviation 0.05 meter is added. To simulate outliers, Gaussian noise with zero mean and standard deviation 3 meters is added to seven samples. Algorithm 2 is applied to 100 data sets of this type, both with an outlier rejection distance of 1 meter and without outlier rejection. Tests have shown that an outlier distance of 5σ or larger is sufficient, where σ is the standard deviation of the noise in input data. Statistics of the root mean square error for the last iteration, $\sqrt{V^k(\mathcal{M})}$, in each example are shown in Figure 3.10. The root mean square errors are more than 5 times higher when the outlier rejection is not applied. The final fit for the data set in the top of Figure 3.10 is shown in the bottom image of Figure 3.10, outlier rejection was applied.

3.5 A Scene Analysis Application

The ground object recognition approach presented in Paper A, is applied in a query-based, multi-sensor vehicle recognition system in Paper E. The approach can also be used for scene analysis [29].

In [29], methods for reconstruction of ground surface, vegetation, buildings, and vehicles are combined to analyze a whole scene. Two examples are presented below. In both examples, data from an airborne, scanning laser radar system are analyzed. A scanning laser radar and a camera are mounted on a helicopter and they register the scene in a down-looking mode. In the examples, the 3D data from the laser radar system are analyzed.

First the bare earth surface is extracted using an active shape model [18, 67]. Trees and large bushes are then detected and measured [61]. The remaining data are searched for large man-made objects such as buildings and smaller ones like vehicles. A data driven approach is used for the building reconstruction [70]. Small clusters of samples of

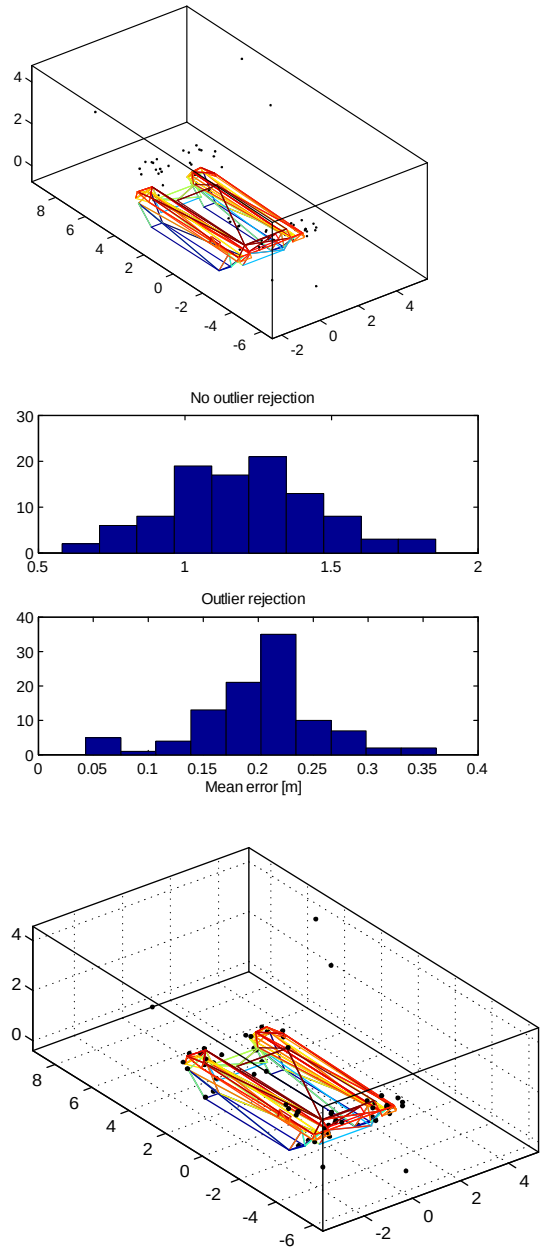

Figure 3.10: *Example of ICP with outlier rejection. Top: Initial fit. Middle: Statistics of final root mean square error for 100 trials. Bottom: Final fit, outlier rejection of 1 meter was applied. Axes in meters.*

proper height and extension are examined by the vehicle recognition module [32]. Further analysis of the remaining, yet unclassified, samples is not included here.

In the first example, see Figure 3.11, there is a T72 tank placed near a building. In the upper right part there is a container and in the lower right there is a tree. The small tree is detected and the building is reconstructed. The container's 3D dimension and orientation are estimated, but they do not match any model in the model library. On the tank, however, there are enough samples to detect the barrel and get a positive match with a low-resolution CAD model of a T72. By estimation of the functional parts of the object, a better result is achieved in the matching step. The result of the analysis of the scene is shown in Figure 3.11C.

In the second example, see Figure 3.12, a tank (T72) is partly hidden under a tree. There are 5-6 trees in the scene. Once the ground surface is estimated and the trees are classified, it becomes easier to analyze the remaining contents. In this case there are fewer samples on the tank and none on the barrel. Thus, only the 3D size and orientation can be estimated.

3.6 Other Approaches to Vehicle Detection

This survey considers different methods for vehicle detection using laser radar data. Detection is defined as a process where a number of samples are identified to have the same features as a typical ground vehicle. Some algorithms of the referred authors can also distinguish objects from non-objects (rocks, trees, image artifacts etc.). The goal of detection is to identify data sets that will be further analyzed for object classification and recognition.

The laser radar data originate from staring systems [86], from scanning systems [2, 5, 20, 53, 82, 87, 90], or from simulations [89, 90]. In [60], the type of sensor system is not described. The resolution of a typical object is usually 100 samples and more, but in [82] there are typically 10-50 samples. The detection approaches usually assume forward-looking (or arbitrary) scene perspective, but in [82] down-looking perspective is considered and in [60] a side-view of the object is assumed. Usually the registration is from one view of the scene only, although in [5, 86] several views are used to get samples from most sides of the vehicles.

A laser radar is a sensor with high angular and depth resolution. This usually means that if large scenes are analyzed, a lot of data have to be processed. In [86], cueing is solved by analyzing 10% of the data set using spin images [45]. In the spin image method, local surface descriptions are generated by transformation of 3D surface points to a 2D representation, called a spin image. The spin image describes the spatial relationship of each point to all other points. To detect the object, a stack of spin images representing the scene are correlated with spin images of object models, stored in a database. The technique is robust to noise and rotation differences. In [89, 90] fast methods that discard the large part of the data set as non-objects are used. In [53, 60, 87] cueing is assumed to be performed by another system (sensor or human), and in [2, 5, 20, 82] the problem is not considered.

Laser sensors typically are subject to dropouts and false alarms, i.e., spurious pixels have unnatural range values. In [20, 53, 60], the detection process can cope with these

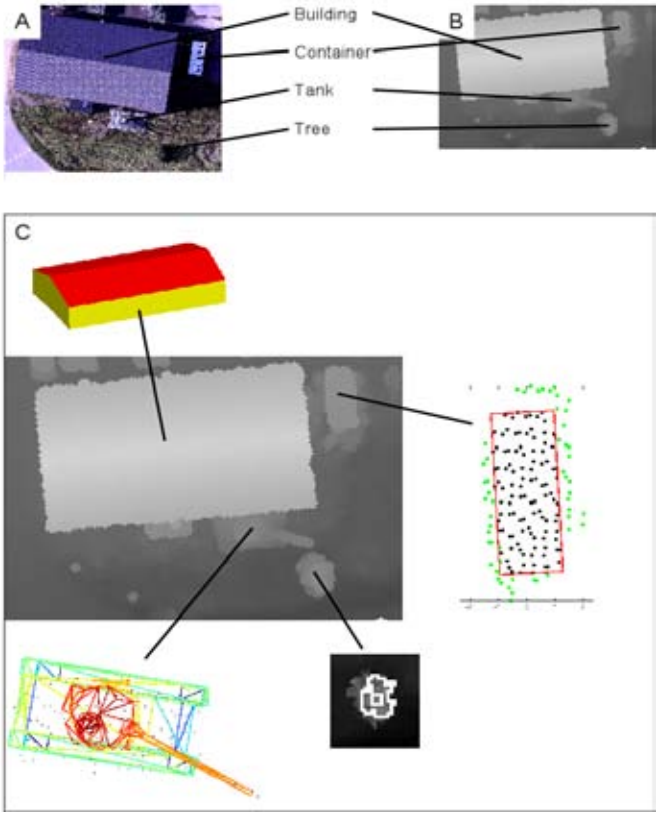

Figure 3.11: *Analysis of a scene containing a tree, a building, a container and a tank. A: Visual (CCD) image, B: Laser radar height data, C: Reconstruction of the scene. The tree, the building, the container, and the tank are marked. In the close-up image of the container the black dots are object samples and the grey dots are ground samples. The rectangle shows the estimated dimensions (meters) of the container.*

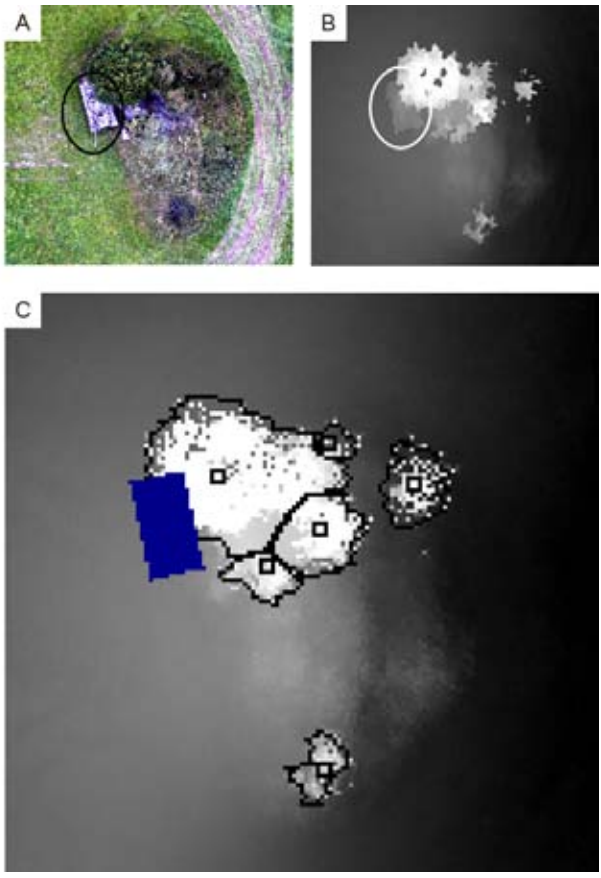

Figure 3.12: *Analysis of a scene containing trees and a partly hidden tank (encircled). A: Visual (CCD) image, B: Laser radar height data, C: Reconstruction of the scene. The contours of the tree crowns and stem positions are marked. The position of the tank is marked with a black box.*

anomalies, while in [87, 90] this problem is taken care of in a preprocessing step. Most of the surveyed papers can deal with several objects in the scene and occlusion, except [87] that assumes that only one object is present in the data set and [82] where occlusion is not a problem due to the application (traffic flow monitoring in down-looking perspective). In some approaches matching with database models is included as a part of the detection process [5, 82, 86]. This results in methods that only can detect objects that are present in the database. The other methods have a filter that marks objects of similar size, or other features, as typical objects. For these methods it is possible to detect new types of vehicles with similar features.

Real time demands are considered in [2, 90]. One of the first steps in the detection methods is to take advantage of the 3D information in data, by height differentiation [20, 53, 82], range segmentation [60, 87, 89], edge detection [2, 90], or shape detection [5, 86]. Several of the methods also contain clustering [20, 53, 90] or, specifically, statistical clustering using connected components [2, 60, 89].

For object detection in open terrain there are robust approaches. The problem with occluded objects is harder to solve. The spin image method is a robust, promising technique but rather slow. Change detection has turned out to be faster in execution time [81], but on the other hand two measurements of the scene at different occasions are necessary. Another interesting approach is combine the 3D and intensity data in the detection process, for example as in Paper F.

3.7 Other Approaches to Vehicle Recognition

This survey is an extension of the survey in Paper A, parts have also been presented in Paper B. Several methods or systems for recognition of military ground vehicles based on laser radar data have been proposed over the years [6, 19, 20, 42, 69, 80, 86, 87, 90, 92], where [69] and [80] describe different parts of the same system. During the recent years, recognition of of civilian cars, mainly for traffic monitoring, has also been presented [39, 82, 91].

The reviewed approaches are applied to data of different resolution and different perspectives of the object. In [6, 20, 69, 82, 90, 91, 92], low resolution data are considered. A typical data set contains up to a few hundred samples, while [82] handles very low-resolution data (approximately 1.5 points/m^2). In [19, 39, 42, 86, 87], there are typically several hundreds of samples on the object. Usually, the data are collected in a forward-looking (or arbitrary) perspective, while in [82] down-looking perspective data are considered, and in [6, 92] side perspective of the vehicle is considered. Data are often obtained using a scanning laser radar system, which results in irregularly sampled data. An exception is [86], where the laser sensor works in staring mode, which gives regularly sampled data. In [42, 69, 92], simulated data is used and in [6] the type of sensor system is not described. Further, in [39, 42, 69, 86], data are collected from several views, which results in data that are less self-occluding. The final result is either a determination of object class (tank, car, truck etc.) [20, 82, 87] or, the more common, object type (tank of type M60, T72 etc.).

In most cases, the recognition process is divided into two steps. Usually the first step consists of fast feature extraction or silhouette calculations [19, 87, 90, 91]. The feature

extraction can retrieve geometrical properties of the object [6, 20, 42, 60, 69], lower-dimensional properties [82, 92], or more abstract features like spin image representation [39, 86]. The first step is used to reduce the list of potential objects. Then, the remaining objects are subject to 3D matching with library models, which usually are represented by CAD models or extracted from registrations of real objects. In [6, 19, 42, 69, 86, 90, 92], the model and object are compared using shape fitting and/or silhouette fitting. In [39, 82, 87], the similarity between model and object is analyzed using rule-based reasoning based on extracted features. In [19, 39, 69, 82], learning approaches are used for the recognition task. In [20], the sample distribution over the object's surface is compared with similar sample distributions generated for models, the orientation of the object relative to the sensor is used. The comparison is accomplished by a $\mathcal{X}^2$ test.

The methods [6, 19, 42, 69, 86, 87, 90] can handle partly occluded objects. The problem with articulated vehicle subparts, for example a rotated barrel on a tank, is handled in a general way in [6, 69, 86, 90] by orientation and dimensions estimations. In [42, 90, 92] one model for each articulated pose is used, resulting in that matching needs to be performed even when the correct type is recognized. The approach in [92] is further evaluated on simulated data in [40]. In [19, 20, 82, 87, 91] the problem with articulated objects is not considered. One reason is that object articulation is not critical when civilian vehicles are considered.

One challenge in object recognition is to use and analyze the object details that are present in laser radar data. Another challenge is the recognition of objects that are partly hidden, i.e., to put the geometrically scattered pieces together into an object. So far, object recognition has been performed on static objects, as only scanning laser radars have been available. Vasile et al. [86] report work on stationary objects where data are collected with a staring system. The staring systems, that collect data in nanoseconds, makes it possible to use 3D laser radars in tracking applications. With the tools reported above, it will be possible to track moving objects and their articulations over time.

3.8 Detection and Recognition of Other Objects

Laser range finders and line scanning laser radars have been used for other purposes than vehicle and mine detection, for example in robot vision and in collision avoidance [41]. In this section, work where 3D and intensity data from laser radars have been used for detection, classification, recognition, or reconstruction of other objects than vehicles and land mines are presented.

Low-resolution 3D laser radar data have been used for mapping of sea bottoms [75, 84], and detection of small objects on the sea bottom [85]. In this case the laser system returned the full waveform of each pulse and the detection was performed using parametric fitting of the waveform.

3D and waveform data can be used for generation of detailed maps of the terrain and urban areas in a fast manner, compared to traditional photogrammetry. See [47, 67] for comparison of ground estimation and building reconstruction methods, respectively. These terrain and urban maps can be used for training and surveillance [71], radio network planning [57], or damage detection and analysis [88]. In [66], outdoor and indoor mapping are combined for modeling and verification of nuclear plant design. In forestry

applications it is important to estimate the wood contents [61]. Gaussian filtering and fitting of a second-order parabolic surface were used to detect the individual trees and estimate their crown diameters and stem positions.

Another area for outdoor and indoor mapping is robot vision. Single point and line scanning laser radars have been used to support passive imaging. In [14, 23], both range images and intensity images are analyzed in parallel and fused afterward. The range images are analyzed using surface fitting and the intensity images' local statistical distribution are analyzed [14]. In [23], objects are detected in both range and intensity images using a cascade of simple classifiers.

Passive imaging is common in face recognition. Problems reported with passive imaging is the sensitivity to registration errors, variation in pose and the illumination effects. In the recent years, face recognition using 3D imaging has been reported with promising results, see [50] for a survey. Lu et al. [56] propose a system that recognizes faces with arbitrary pose. Several 2.5D images are combined to retrieve a 3D image of the face. The recognition process is based on surface matching using ICP for the 3D data and the intensity images are analyzed using projection techniques (linear discriminant subspace analysis). In [17], faces are detected using curvature matching of salient facial features. For recognition, 3D and 2D images of the face are combined and a classifier based on principle component analysis separates face and non-faces. In [72], 3D models of faces are constructed using laser radar data. To recognize a person, a range image, of the same pose as the input range image, is generated from the 3D model. The range images are matched using correlation.

In industry applications 3D imaging has been used for precise inspection where it is hard for humans to detect failures, and for repetitive, heavy or dangerous tasks which are unsuitable for humans. In [63], 3D imaging is used for detection and measurement of flank wear in a cutting tool machine, and in [65] laser radar data are used for failure detection in piston production. In these cases, the level of detail is thousands times smaller than in the other reported applications, μm-precision is necessary. To detect if there is flank wear present on the tool, a 3D image of the tool is produced and the cross-sections are analyzed using peak detection. In [65], the authors claim that it is not necessary to reconstruct the 3D shape. The failures in the pistons are detected using least squares fitting of key reference points.

In another group of applications, a laser radar is placed on a robot to retrieve robot vision or support the operator in planning the robot's operation. 3D and intensity data have been used for fruit harvesting [44]. The fruit that is collected by the robot is apples and the signal processing detects primitives typical for spherical objects (convex surfaces, contours, etc.) in range and intensity data. The primitives are used to be able to cope with the non-structural background and partly occluded objects. The detected primitives are analyzed in parallel and finally the fruit is recognized using sphere fitting. Partly occluded objects are also a problem in a box depalletizing application [48]. The boxes are detected by their edges and a vertex describing the visual edges of the box. Once stable features are detected, the box candidates are compared to box templates using geometric fitting. In the last application, a laser radar scanner is used to build a 3D model of the robot's working environment [36]. The working tasks are in environment restoration and waste management and the scene's geometry is highly unstructured or uncertain. In this case spin images and ICP are used to build a reliable 3D model of the working scene.

The trend is that 3D laser radar systems become less expensive, faster and smaller in size, which will encourage usage in various fields. When staring laser radars become more widely available, the measurement technique will find its way into new applications. In face recognition, the scene in measurement situation can be controlled, but the human may move during the data capture. With faster sensor systems, this will be less of a problem. In robot vision for outdoor scenes, ware-house applications, and fruit harvesting, the scene is less controlled. There are similarities with recognition of vehicles and land mines placed in urban or natural environments and also, similar signal processing approaches are used.

4

Performance Analysis

When developing signal and image processing methods it is important to have knowledge of the uncertainty sources in the measurement system. The uncertainty sources are typically described in error and noise models. Further uncertainties in data can be introduced during resampling. Once the accuracy in measurement data is modeled, the next question is the performance of the overall recognition system, i.e., the accuracy of both the measurement system and the recognition algorithm that process data.

Performance of laser radar systems is discussed in Papers C- D. Parts of the contents in this chapter have earlier been presented in [29]. In this chapter, first a survey of methods for performance analysis of laser radar systems is presented. In Section 4.2, the Cramér-Rao lower bounds for the cases when data are subject to white Gaussian noise, and the case for general Gaussian noise are presented. The models for laser radar systems used in this thesis are presented in Section 4.3. In the last section, Section 4.4, the Cramér-Rao lower bound expressions for range and intensity data are presented.

4.1 Performance analysis of laser radar systems

Modeling of a complete recognition system is rather difficult, as there are several nonlinearities and different statistical distributions involved. The most straightforward way is to collect thousands of data sets in a field campaign and then run the algorithms on the data sets. A protocol for evaluation of 3D imaging laser radar systems in field tests is proposed in [59]. Often complete field tests are too expensive, leading to the more common way of combining field tests with simulations. Algorithms can be analyzed by benchmarking using common data sets. This is common in the 2D imaging community, for 3D imaging open databases are not yet common. To simulate the object recognition process, a model of the measurement system and a method to analyze the performance of the algorithm are needed. Usually, an expression of the best possible system performance is wanted.

In [3], typical measurement uncertainty sources of laser radar systems for industrial applications are described. The main sources are the electronic components in the transmitter and receiver systems, the laser range finder (in a time-of-flight measuring systems), and speckles induced at the object's surface. These sources of uncertainties are, in our perspective, more applicable when designing a sensor than when using a sensor system outdoors.

For outdoor applications the sources of measurement uncertainties described in [24, 34, 77] are more applicable. The authors model general direct-detection laser radar systems, applicable for both scanning and staring approaches. In this case the transmitter is assumed to be ideal and the main sources of uncertainties are the atmosphere, the object, and the receiver system. In the atmosphere, the diffraction, turbulence, scintillations, and attenuation due to aerosols are the main sources. At the object, the object's geometry, speckles, and specular and diffuse reflectance affect the laser beam. At the receiver the main sources of uncertainty are backscatter from the transmitter equipment and aerosols, solar background radiation, and, finally, the optical and electronic components in the receiver. A model of a general coherent laser radar for outdoor usage is proposed in [25, 26]. Gerwe et al. [24] model the properties of the laser radar intensity image, while in [25, 26, 34, 77] the properties in the range image are modeled. All models are based on sensor physics and statistical properties of sensors, object interaction, background, and atmosphere.

Once the measurement system is properly modeled, the performance of the overall system must be analyzed. Many authors assume or show that their estimation algorithm is optimal [24, 28, 51, 73], for example in [24, 73] optimal Bayesian-based recognition methods are proposed. Evaluation of a non-optimal algorithm is presented in [25, 26]. There are various theoretical bounds reported. Among them the Cramér-Rao Lower Bound (CRLB) is common [24, 26, 28, 34]. The CRLB is described in Section 4.2. In [51, 73], the Hilbert-Schmidt bound is used. The Hilbert-Schmidt bound gives the lower bound on the estimation error associated with any estimator that can handle rotations and translations, it is a generalization of the CRLB. By using statistical detection theory the performance can be evaluated using Neuman-Pearson's criterion [25] or the complete data bound [26].

4.2 The Cramér-Rao lower bound

It is always desirable to understand how a particular estimation scheme performs under a certain model. If a distribution of the perturbations is defined, a lower bound on the error covariance of the estimated parameters can be calculated using the Cramér-Rao lower bound [49, 55]. The CRLB states the lower limit of any minimum variance and unbiased estimator in terms of its mean square error. The lower limit can be reached if the estimator is minimum variance and unbiased [49]. For a parameter vector $\theta = (\theta_1, \theta_2, ..., \theta_K)^t$, the CRLB is written

$$E\left(\theta^0 - \hat{\theta}\right)\left(\theta^0 - \hat{\theta}\right)^t \geq J^{-1}(\theta),$$

where $E(\cdot)$ is the expectation operator, θ^0 is the true value, $\hat{\theta}$ its estimate, and J is the Fisher Information Matrix (FIM). The FIM is representing the information obtained in

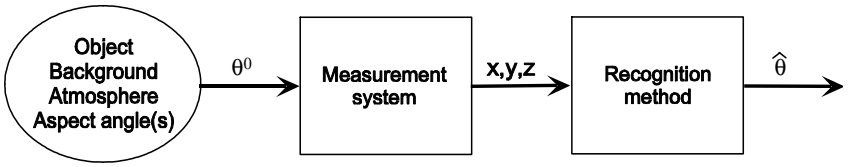

Figure 4.1: *Model of a general laser radar system. The ellipse to the left symbolizes the atmospheric affects and the object's surface structure and shape, which affects the laser beam. The middle box describes the measurement system and the right box the algorithm used for data analysis.*

data. The CRLB can be calculated analytically or numerically in Monte Carlo simulations.

For a measurement vector $x = (x_1, x_2, ..., x_N)^t$, the probability density function for obtaining x given the parameters θ is denoted $p(x \mid \theta)$. For an unbiased estimator, $E(\hat{\theta}) = \theta$, the FIM is a $K \times K$ matrix with [49]

$$J(\theta)_{ij} = -E\frac{\partial^2 \ln p(x \mid \theta)}{\partial\theta_i \partial\theta_j}. \tag{4.1}$$

For the case when x is Gaussian distributed but contains bias, i.e.,

$$x \in \mathcal{N}(\mu(\theta), \Sigma(\theta)), \tag{4.2}$$

the elements in the FIM are given by

$$J(\theta)_{ij} = \left(\frac{\partial\mu(\theta)}{\partial\theta_i}\right)^t \Sigma^{-1}(\theta)\left(\frac{\partial\mu(\theta)}{\partial\theta_j}\right) + \frac{1}{2}\mathrm{tr}\left(\Sigma^{-1}(\theta)\left(\frac{\partial\Sigma(\theta)}{\partial\theta_i}\right)\Sigma^{-1}(\theta)\left(\frac{\partial\Sigma(\theta)}{\partial\theta_j}\right)\right), \tag{4.3}$$

where

$$\frac{\partial\mu(\theta)}{\partial\theta_i} = \left(\frac{\partial[\mu(\theta)]_1}{\partial\theta_i}, \frac{\partial[\mu(\theta)]_2}{\partial\theta_i}, \ldots, \frac{\partial[\mu(\theta)]_N}{\partial\theta_i}\right), \tag{4.4}$$

and

$$\frac{\partial\Sigma(\theta)}{\partial\theta_i} = \begin{pmatrix} \frac{\partial[\Sigma(\theta)]_{11}}{\partial\theta_i} & \frac{\partial[\Sigma(\theta)]_{12}}{\partial\theta_i} & \cdots & \frac{\partial[\Sigma(\theta)]_{1N}}{\partial\theta_i} \\ \frac{\partial[\Sigma(\theta)]_{21}}{\partial\theta_i} & \frac{\partial[\Sigma(\theta)]_{22}}{\partial\theta_i} & \cdots & \frac{\partial[\Sigma(\theta)]_{11}}{\partial\theta_i} \\ \vdots & \vdots & \ddots & \vdots \\ \frac{\partial[\Sigma(\theta)]_{N1}}{\partial\theta_i} & \frac{\partial[\Sigma(\theta)]_{N2}}{\partial\theta_i} & \cdots & \frac{\partial[\Sigma(\theta)]_{NN}}{\partial\theta_i} \end{pmatrix}. \tag{4.5}$$

4.3 Models of Laser Radar Systems

In Figure 4.1, a typical system for object recognition is illustrated. The (unknown) object's features, e.g., length, and orientation, are described by θ. The measurement system,

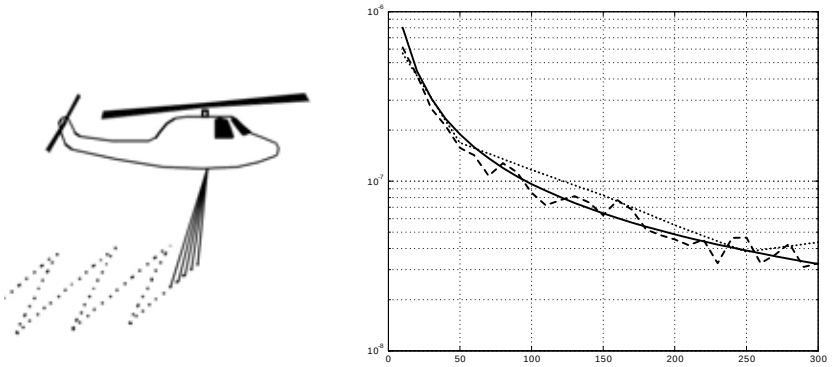

Figure 4.2: *Left: An airborne laser radar scanner, the scan pattern is shown. Right: Validation of the models.* $Var\left(n_1^0 - \hat{n}_1\right)$ *as a function of the number of samples* N *is shown. Solid: CRLB, dashed: MSE from a simulation of the measurement error model, dotted: MSE from a simulation of the measurement system.*

here a laser radar, registers some phenomena at the object in the variables $\varphi_i = (x, y, z, I)_i$, where $i = 1, ..., N$ are the samples. The analysis method processes the variables and estimates the features in $\hat{\theta}$.

In Paper D, a model of a down-looking, helicopter-carried, scanning laser radar system is analyzed. The laser radar system is connected to a Global Positioning System (GPS) and the laser samples are fused with the GPS coordinates. Each sample contains (x, y, z, I), where (x, y) is the position, z is the altitude, and I is the intensity in the returned pulse. This means that the data set corresponds to a 3D mapping of the terrain. Define the regression vector

$$\varphi = (x, y, z, I)\,.$$

This regression vector φ can also be expressed as function of the measurement system

$$\varphi = f\left(R, \alpha_{scan}, \alpha_{pitch}\right),$$

where R is the slant range distance measured by the laser range finder in a certain scan angle, α_{scan}, and pitch angle, α_{pitch}. Implicitly, φ is also a function of the object's shape, atmosphere, receiver, detector properties, etc. This model is in Paper D compared with a measurement error model for line estimation. The relation between the number of samples N and the estimation performance of the line orientation n_1, is shown in Figure 4.2. The measurement error model is minimum variance and therefore close to the CRLB limit. The data from the simulated laser radar system is also close to the CRLB.

In Paper C, the left and middle boxes in Figure 4.1 are described in detail, see Figure 4.3. This model is used to analyze the uncertainties in range estimation. The laser signal transmitted from the laser, $S_s\left(x, y, t\right)$, is after interaction with the object, the atmosphere, and the receiver returned as $S_r\left(x, y, t\right)$. The factors included in this model are the object's shape and surface structure, object-induced speckles (F_{speckle}), turbulence-induced scintillations and beam pointing error (F_{scint}) due to the atmosphere, laser and

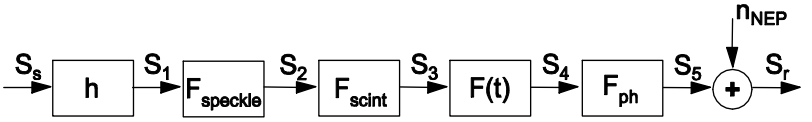

Figure 4.3: *Model of a general, direct-detection laser radar system.*

receiver properties ($F(t)$), the transformation from photons to electrical current in the receiver (F_{ph}), and the noise sources in the detector (n_{NEP}). The estimated object range is considered a function of $S_r\left(x,y,t\right)$, i.e.,

$$\hat{R}\left(x,y\right)=f_1\left(S_r\left(x,y,t\right)\right). \tag{4.6}$$

The range data is also used for shape fitting, where the parameter vector θ describes the estimated shape:

$$\hat{\theta}=f_2\left(\hat{R}\left(x,y\right)\right). \tag{4.7}$$

In Paper C, the range errors generated in different types of receivers are analyzed. Receivers using peak detection, constant fraction detection, or matched filter are studied. Measurements on a plane, a cone, a sphere, and a parabola are simulated using the model in Figure 4.3. As an example, the estimated range errors for a plane are shown in Figure 4.4. When the slope angle of the plane, ϕ_x, increases, the laser beam is broadened and the range error increases. The properties of the range error vary with the detection method, with the lowest range error obtained for the matched filter. It is concluded in Paper C that the estimation of range can be modeled as

$$\hat{R}=R_0+\Delta R, \tag{4.8a}$$

$$\Delta R\in\mathcal{N}\left(b\left(\theta\right),\sigma_{\hat{R}}^2\left(\theta\right)\right), \tag{4.8b}$$

where R_0 is the true but unknown range, the bias b and variance $\sigma_{\hat{R}}^2$ vary with the object's shape, θ, and signal-to-noise ratio. If an optimal signal detector, like the matched filter, is used in the receiver the bias is close to zero.

4.4 CRLB expressions for laser radar data

Let us study the model of a direct-detection laser radar in the CRLB framework a bit closer. Using the notation of Section 4.3, the intensity estimate $\hat{I}$ is calculated from the received pulse S_r. If the sensor elements in the detector are assumed to be statistically independent, the intensity values in sensor element (x,y) can be modeled as [24]

$$\hat{I}\left(x,y\right)=\text{Po}\left(S_r\left(x,y,t\right)\right)+n_I, \tag{4.9a}$$

$$n_I\in\mathcal{N}\left(0,\sigma_I^2\right), \tag{4.9b}$$

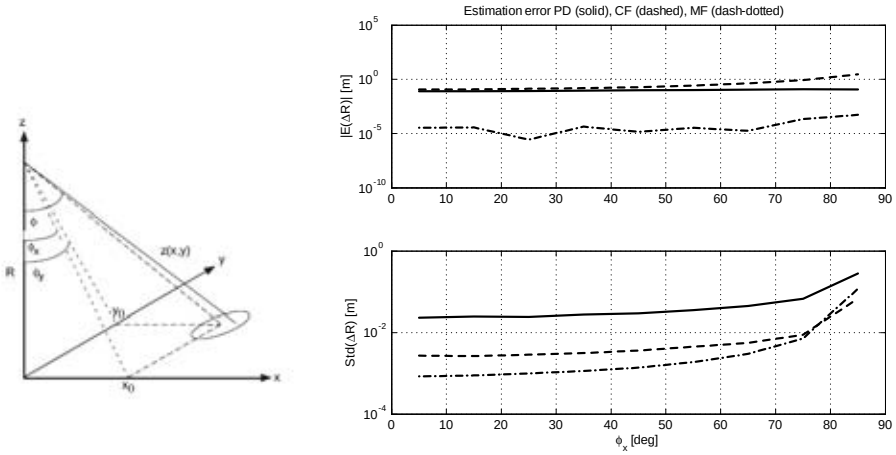

Figure 4.4: *Left: Geometry for the plane surface. Right: The mean, $|E(\Delta R)|$, and standard deviation, std(ΔR), of the range error, ΔR, as a function of slant angle, ϕ_x. Solid: peak detection, dashed: constant fraction, dash-dotted: matched filter.*

where Po(x) is a Poisson distributed random variable with mean x, and n_I is a zero-mean Gaussian random variable with standard deviation σ_I. This model is also used for passive imaging, like visual and IR cameras [68]. The uncertainty in intensity value is $\Delta I = \hat{I} - I^0$, where I^0 is the true value. The uncertainty in intensity value in pixel (x, y) can be modeled [24]

$$\Delta I(x,y) = \text{Po}\left(S_r(x,y,t) + \sigma_I^2\right) - \sigma_I^2,$$

and the elements in the FIM is given in [24]

$$J(\theta)_{ij} = \frac{\frac{\partial S_r(x,y,t|\theta)}{\partial \theta_i}\frac{\partial S_r(x,y,t|\theta)}{\partial \theta_j}}{S_r(x,y,t \mid \theta) + \sigma_I^2}, \tag{4.10}$$

where the denominator is the noise variance in pixel (x, y). The uncertainty in range estimation in pixel (x, y) is modeled

$$\Delta R(x,y) \in \mathcal{N}\left(b(x,y \mid \theta), \sigma_R^2(x,y \mid \theta)\right), \tag{4.11}$$

and the CRLB expression (4.3) apply.

These expressions give the complete statistical distribution for laser radar data. The model of the range data give us the opportunity to analyze the performance within the same framework as passive imaging systems. The expressions of the CRLB are usually too complicated to compute analytically and instead simulations can be used, see for example Papers C- D. In Paper D, the range uncertainty was not known and the range data was achieved using ray tracing calculations on subpixel level for the entire scene. With this model, the estimated range can be received from (4.3) and applied to simple scenes

without ray tracing calculations. The proposed statistical model of the range error seems easy, as it is Gaussian distributed, but the expression of the range uncertainty becomes complicated if the object or the scene consists of more complex shapes than a plane or a sphere. A simplification can be to divide the scene into a few surface primitives, and calculate the bias and variance for these surfaces. This must, however, be subject to further studies.

5

Summary

The focus in this thesis is object detection and recognition using laser radar data. A laser radar captures high-resolution data where details of the objects are resolved. A method where the parts of the objects are identified is proposed. To analyze the performance, modeling of laser radar system was performed. Performance issues are discussed in terms of the Cramér-Rao lower bound.

5.1 Ground object detection and recognition

In Paper F, a Bayesian approach to object/background segmentation and object clustering is proposed. Both range and intensity data were used simultaneously. The method could segment and cluster data in an example, while unsatisfactory results were received if only range or intensity data was used. The results are promising, but the method must be studied further.

The core in the object recognition method is rectangle matching. Nine approaches to object dimension and orientation estimation, based on rectangle estimation, are presented in Paper F. The estimator's parameter estimation accuracy and execution time are compared in Monte Carlo simulations. The minimization of the rectangle's area, that is used in the object recognition method, showed to have good over-all performance.

A ground object detection method based on 3D laser radar data is presented in Paper A. The method handles general, irregularly sampled 3D data. It is based on the fact that man-made objects of complex shape can be decomposed to a set of rectangles. The method consists of four steps; 3D size and orientation estimation, object segmentation into parts of approximately rectangular shape, identification of segments that represent the object's functional/main parts, and object matching with CAD models. The method is tested on vehicle data, collected with four fundamentally different laser radar systems. The matching of all objects with all models resulted in some confusion within the object

class. There was no confusion between the three object classes. The method is tested on data from field experiments, although the number of examples is rather low (33 vehicles in total), we believe that it is promising.

In Paper B, the interaction between the object recognition method and the model library is further analyzed. An approach to 3D content-based model matching that utilizes efficient geometric feature extraction is proposed. The matching method takes articulations into account. The geometric features are matched with the model descriptors, to gain fast and early rejection of non-relevant models. A sequential matching is used, where the number of functional parts increases in each iteration. The division into parts increases the possibility for correct matching results when several similar models are available. An iterative, modular, least squares method for matching of point scatter and face models that include outlier rejection is proposed. The method falls within the iterative closest point framework. The paper also presents a penalty function that is used for selection of the number of functional parts. The approach is exemplified with a vehicle recognition application, where some vehicles have functional parts.

5.2 Performance analysis

In Paper C, a model of a general direct-detecting laser radar system applicable for hard-target measurements is presented. The laser radar cross sections, i.e., the impulse response of the laser beam's object interaction, are derived for some simple geometric shapes (plane, cone, sphere, and parabola). The cross section models are used, in simulations, to find the statistical distribution of uncertainties in time-of-flight estimations. Three time-of-flight estimation algorithms are analyzed; peak detection, constant fraction detection, and matched filter. The detection performance for various shape conditions and signal-to-noise ratios is analyzed. The Cramér-Rao lower bound is derived and the detector's performances are compared with that bound. The laser radar system is described in a channel model context, which clarifies the system's properties from a signal processing view. The detector with best performance is the matched filter, the time-of-flight estimate have lower variance and a bias that is close to zero. It is shown that the range error can be modeled as Gaussian distributed, with bias and variance that are functions of object shape and signal-to-noise ratio.

In Paper D, a tool for synthetic generation of scanning laser radar data is described and its performance is evaluated. By analyzing the synthetic data, performance of detection and recognition algorithms can be performed. In the measurement system model it is possible to change and add several design parameters, which makes it possible to test an estimation scheme under different types of system design. The measurement system model includes laser characteristics, object geometry, reflection, speckles, atmospheric attenuation, turbulence, and a direct-detection receiver. A parametric method that estimates an object's size and orientation is described. There are measurement errors present and thus, the parameter estimation is based on a measurement error model. The Cramér-Rao lower bound for line estimation under the presence of measurement errors is derived. It is shown in simulations that both the laser radar model and the measurement error model are close to the Cramér-Rao lower bound.

5.3 Applications

A query-based system for ground object recognition based on multi-sensor data is presented in Paper E. The system covers the complete process for automatic ground object recognition, from sensor data to the user interface, i.e., from low-level image processing to high-level situation analysis. The system is based on a query language and a query processor, and includes object detection, object recognition, data fusion, presentation and situation analysis. The object recognition is executed in sensor nodes, each containing a sensor and the corresponding signal/image processing algorithms. Promising results using infrared and laser radar data are reported, demonstrating the capabilities of the object recognition algorithms, the advantage of the two-level data fusion, and the query-based system. The division of the object recognition into two steps improve performance, and decrease computational complexity. The system's modular architecture and the computational model simplify insertion of new algorithms and/or sensor types.

Bibliography

[1] J. Ahlberg, M. Folkesson, C. Grönwall, T. Horney, E. Jungert, L. Klasén, and M. Ulvklo. Ground target recognition in a query-based multi-sensor information system. *To be submitted*, 2006.

[2] E. Al-Hujazi and A. Sood. Range image segmentation with applications to robot bin-picking using vacuum gripper. *IEEE Transactions on Systems, Man and Cybernetics*, 20(6):1313–1324, 1990.

[3] M.-C. Amann, T. Bosch, M. Lescure, R. Myllylä, and M. Rioux. Laser ranging: A critical review of usual techniques for distance measurement. *Optical Engineering*, 40(1):10–19, 2001.

[4] P. Andersson. Long range 3D imaging using range gated laser radar images. *Optical Engineering*, 45(3), 2005.

[5] D. Anguelov, B. Taskar, V. Chatabashev, D. Koller, D. Gupta, G. Heitz, and A. Ng. Discriminative learning of markiv random fileds for segmentation of 3D scan data. In *IEEE Conference on Computer Vision and Pattern Recognition*, volume 2, pages 169–176, San Diego, CA, June 2005.

[6] W. Armbruster. Comparison of deterministic and probabilistic model matching techniques for laser radar target recognition. In *Proceedings SPIE*, volume 5807, pages 233–240, May 2005.

[7] K.S. Arun, T.S. Huang, and S.D. Blostein. Least-squares fitting of two point sets. *IEEE Transactions on Pattern Analysis and Machine Intelligence*, 9(5):698–700, 1987.

[8] P.J. Besl and N.D. McKay. A method for registration of 3-D shapes. *IEEE Transactions on Pattern Analysis and Machine Intelligence*, 14(2):239–256, 1992.

[9] A.P.W. Bowman, E.M. Stocker, and A.D. Lucey. Hyperspectral infrared techniques for buried landmine detection. In *Proceedings of the Second International Conference on Detection of Abandoned Land Mines*, Edinburgh, UK, October 1998.

[10] C. Carlsson. Vehicle size and orientation estimation using geometric fitting. Technical Report Licentiate Thesis no. 840, Department of Electrical Engineering, Linköping University, Linköping, Sweden, June 2000.

[11] C. Carlsson, E. Jungert, C. Leuhusen, D. Letalick, and O. Steinvall. A comparative study between two target detection methods applied to ladar data. In *Proceedings of the 9th Conference on Coherent Laser Radar*, pages 220–223, Linköping, Sweden, June 1997.

[12] C. Carlsson, E. Jungert, C. Leuhusen, D. Letalick, and O. Steinvall. Target detection using data from a terrain profiling laser radar. In *Proceedings of the 3rd International Airborne Remote Sensing Conference and Exhibition*, pages I–431 – I–438, Copenhagen, Denmark, July 1997.

[13] C. Carlsson and M. Millnert. Vehicle size and orientation estimation using geometric fitting. In *Proceedings SPIE*, volume 4379, pages 412–423, Orlando, April 2001.

[14] C.-C. Chu, N. Nandhakumar, and J.K. Aggarwal. Image segmentation using laser radar data. *Pattern Recognition*, 23(6):569–581, 1990.

[15] S.K. Clark, W.D. Aimonetti, F. Roeske, and J.G. Donetti. Multispectral image feature selection for land mine detection. *IEEE Transactions on Geoscience and Remote Sensing*, 38:304–311, 2000.

[16] L.M. Collins, L.G. Huettel, W. A. Simpson, and S.L. Tantum. Sensor fusion of EMI and GPR data for improved land mine detection. In *Proceedings SPIE*, volume 4742, pages 872–879, August 2002.

[17] A. Colombo and C. Cusano. A 3D face recognition system using curvature-based detection and holistic multimodal classification. In *Proceedings of the 4th International Symposium on Image and Signal Processing and Analysis*, pages 179–84, September 2005.

[18] M. Elmqvist. Ground estimation of laser radar data using active shape models. In *OEEPE Workshop on Airborne Laserscanning and Interferometric SAR for Detailed Digital Elevation Models*, Stockholm, Sweden, March 2001.

[19] C. English, S. Ruel, L. Melo, P. Church, and J. Maheux. Development of a practical 3D automatic target recognition and pose estimation algorithm. In *Proceedings SPIE*, volume 5426, pages 112–123, September 2004.

[20] R.Ll. Felip, S. Ferredans, J. Diaz-Caro, and X. Binefa. Target detection in LADAR data using robust statistics. In *Proceedings SPIE*, volume 5988, pages 160–170, October 2005.

[21] M. Folkesson, C. Grönwall, and E. Jungert. A fusion approach for coarse-to-fine target recognition. In *Proceedings SPIE*, volume 6242, page 62420H, April 2006.

[22] H. Freeman and D. Shapira. Determining the minimum-area encasing rectangle for an arbitrary closed curve. *Communications of the ACM*, 18(7):409–413, 1975.

[23] S. Frintrop, E. Rome, A. Nuchter, and H. Surmann. A bimodal laser-based attention system. *Computer Vision and Image Understanding*, 100:124–151, 2005.

[24] D.R. Gerwe and P.S. Idell. Cramér-Rao analysis of orientation estimation: Viewing geometry influences on the information conveyed by target features. *Journal of Optical Society of America A*, 20(5):797–816, May 2003.

[25] T.J. Green and J.H. Shapiro. Detecting objects in three-dimensional laser radar images. *Optical Engineering*, 33(3):865–874, 1994.

[26] D.R. Greer, I. Fung, and J.H. Shapiro. Maximum-likelihood multiresolution laser radar range imaging. *IEEE Transactions on Image Processing*, 6(1):36–46, 1997.

[27] C. Grönwall, P. Andersson, and F. Gustafsson. Least squares fitting of articulated objects. In *Workshop on Advanced 3D Image Analysis For Safety and Security, Proceedings of IEEE Conference on Computer Vision and Pattern Recognition*, pages 116–121, San Diego, CA, June 2005.

[28] C. Grönwall, T. Carlsson, and F. Gustafsson. Performance analysis of measurement error regression in direct-detection laser radar imaging. In *Proceedings IEEE Conference on Acoustics, Speech and Signal Processing*, volume VI, pages 545–548, Hong Kong, April 2003.

[29] C. Grönwall, T. Chevalier, Å. Persson, M. Elmqvist, S. Ahlberg, L. Klasén, and P. Andersson. Methods for recognition of natural and man-made objects using laser radar data. In *Proceedings SPIE*, volume 5412, pages 310–320, April 2004.

[30] C. Grönwall and F. Gustafsson. 3D content-based model matching using geometric features. *Submitted to Pattern Recognition*, 2006.

[31] C. Grönwall and F. Gustafsson. Approaches to Object/Ground segmentation and object dimension estimation. Technical Report LiTH-ISY-R-2746, Dept. Electrical Engineering, Linköpings Universitet, Linköping, Sweden, 2006.

[32] C. Grönwall, F. Gustafsson, and M. Millnert. Ground target recognition using rectangle estimation. *Accepted for publication in IEEE Transactions on Image Processing*, 2006.

[33] C. Grönwall, F. Gustafsson, and M. Millnert. Ground target recognition using rectangle estimation. Technical Report LiTH-ISY-R-2684, Dept. of Electrical Engineering, Linköpings Universitet, Linköping, Sweden, 2006.

[34] C. Grönwall, O. Steinvall, F. Gustafsson, and T. Chevalier. Influence of laser radar sensor parameters on range measurements and shape fitting uncertainties. *Submitted to Optical Engineering*, 2006.

[35] I.Y.-H. Gu and T. Tjahjadi. Detecting and locating landmine fields from vehicle- and air-borne measured IR images. *Pattern Recognition*, 35:3001–3014, 2002.

[36] W.R. Hamel and R.L. Kress. Elements of telerobotics necessary for waste clean up automation. In *Proccedings of IEEE International Conference on Robotics and Automation*, volume 1, pages 393–400, May 2001.

[37] H.T. Haskett, D.A. Reago, and R.R. Rupp. Detectability of buried mines in 3-4 micrometers and 8-12 micrometers regions for various soils using hyperspectral signatures. In *Proceedings SPIE*, volume 4394, pages 296–309, October 2001.

[38] T. Horney, J. Ahlberg, C. Grönwall, M. Folkesson, K. Silvervarg, J. Fransson, L. Klasén, E. Jungert, F. Lantz, and M. Ulvklo. An information system for target recognition. In *Proceedings SPIE*, volume 5434, pages 163–175, April 2004.

[39] D. Huber, A. Kapuria, R. Donamukkala, and M. Hebert. Parts-based 3D object classification. In *IEEE Conference on Computer Vision and Pattern Recognition*, volume 2, pages II–82 – II–89, June-July 2004.

[40] B.A. Hutchinson, R.L. Galbraith, B.L. Stann, and S.Z. Der. Simulation-based analysis of range and cross-range resolution requirements for the identification of vehicles in ladar imagery. *Optical Engineering*, 42(9):2734–2745, 2003.

[41] J. Jansson. *Collision Avoidance Theory with Application to Automotive Collision Mitigation*. PhD thesis, Linköping Studies in Science and Technology, Dept. of Electrical Engineering, Linköping University, Linköping, Sweden, June 2005.

[42] M. A. Jeffris. Robust 3D ATR techniques based on geometric invariants. In *Proceedings SPIE*, volume 5807, pages 190–200, May 2005.

[43] A.V. Jelalian. *Laser Radar Systems*. Artech House, Norwood, MA, 1992.

[44] A.R. Jiménez, R. Ceres, and J.L. Pons. A vision system beased on a laser rangefinder applied to robotic fruit harvesting. *Machine Vision and Applications*, 11: 321–329, 2000.

[45] A.E. Johnson and M. Hebert. Using spin images for efficient object recognition in cluttered 3D scenes. *IEEE Transactions on Pattern Analysis Machine Intelligence*, 21(5):433–449, 1999.

[46] E. Jungert, C. Carlsson, and C. Leuhusen. A qualitative matching technique for handling uncertainties in laser radar images. In *Proceedings SPIE*, volume 3371, pages 62–71, September 1998.

[47] H. Kaartinen, J. Hyyppä, E. Gülch, G. Vosselman, H. Hyyppä, L. Matikainen, A.D. Hofmann, U. Mäder, Å. Persson, U. Söderman, M. Elmqvist, A. Ruiz, M. Dragoja, D. Flamanc, G. Maillet, T. Kersten, J. Carl, R. Hau, E. Wild, L. Frederiksen, J. Holmgaard, and K. Vester. Accuracy of 3D city models: EuroSDR comparison. In *Proceedings ISPRS Working Groups III/3, III/4, V/3 Workshop "Laser Scanning 2005"*, Enschede, the Netherlands, September 2005.

[48] D. Katasoulas and L. Bergen. A versatile depalletizer of boxes based on range imagery. In *Proceedings of IEEE International Conference on Robotics and Automation*, pages 4313–4319, Washington, DC, May 2002.

[49] S.M. Kay. *Fundamentals of Statistical Signal Processing: Estimation Theory*, volume 1. Prentice Hall, Upper Saddle River, NJ, 1993.

[50] J. Kittler, A. Hilton, M. Hamouz, and J. Illingworth. 3D assisted face recognition: A survey of 3D imaging, modelling and recognition approaches. In *Proceedings of IEEE Conference on Computer Vision and Pattern Recognition*, pages 114 – 114, San Diego, CA, June 2005.

[51] A.E. Koksal, J.H. Shapiro, and M.I. Miller. Performance analysis for ground-based target orientation estimation: FLIR/LADAR sensor fusion. In *Conference Record of the Thirty-Third Asilomar Conference on Signals, Systems, and Computers*, volume 2, pages 1240 –1244, October 1999.

[52] D. Letalick, J. Ahlberg, P. Andersson, T. Chevalier, C. Grönwall, H. Larsson, Å. Persson, and L. Klasén. 3-D imaging by laser radar and applications in preventing and combating crime and terrorism. In *NATO RTO SCI Symposium on Systems, Concepts and Integration (SCI) Methods and Technologies for Defence Against Terrorism*, volume RTO-MP-SCI-158, London, UK, October 2004.

[53] D. Letalick, M. Millnert, and I. Renhorn. Terrain segmentation using laser radar range data. *Applied Optics*, 31(15):2882–2890, 1992.

[54] A. Linderhed, S. Sjökvist, S. Nyberg, M. Uppsäll, C. Grönwall, P. Andersson, and D. Letalick. Temporal analysis for land mine detection. In *Proceedings of the 4th International Symposium on Image and Signal Processing and Analysis (ISPA)*, Zagreb, Croatia, September 2005.

[55] L. Ljung. *System Identification. Theory for the User.* Prentice Hall, NJ, 2nd edition, 1999.

[56] X. Lu, A.K. Jain, and D. Colbry. Matching 2.5D face scans to 3D models. *IEEE Transactions on Pattern Analysis and Machine Intelligence*, 28(1):31–43, 2006.

[57] H.-G. Maas and G. Vosselman. Two algorithms for extracting building models from raw laser altimetry data. *ISPRS Journal of Photogrammetry and Remote Sensing*, 54:153–163, 1999.

[58] P.L. Martínez, L. Von Kempen, H. Sahli, and D.C.Ferrer. Improved thermal analysis of buried landmines. *IEEE Transactions on Geoscience and Remote Sensing*, 42: 1965–1975, 2004.

[59] B.H. Miles, J.E. Land, A.L. Hoffman, W.R. Humbert, B.A. Smith, A.B. Howard, J.L. Cox, M.S. Foster, D. Onuffer, S.L. Thompson, T. Ramrath, C.E. Harris, and P. Freedman. Field testing protocols for evaluation of 3d imaging focus plane array ladar systems. In *Proceedings SPIE*, volume 4723, pages 43–56, July 2002.

[60] J. Neulist and W. Armbruster. Segmentation, classification and pose estimation of military vehicles in low resolution laser radar images. In *Proceedings SPIE*, volume 5791, pages 218–225, May 2005.

[61] Å. Persson, J. Holmgren, and U. Söderman. Detecting and measuring individual trees using an airborne laser scanner. *Photogrammetric Engineering and Remote Sensing*, 68(9):925–932, 2002.

[62] H. Pirzadeh. Computation geometry with the rotating calipers. Master's thesis, Faculty of Graduate Studies and Research, McGill University, Canada, Nov 1999.

[63] O. Ryabov and K. Mori. Laser sensor for imaging and detection of cutting tool wear. In *Proceedings of the ISA/IEEE Sensors for Industry Conference*, pages 44–46, Huston, TX, November 2002.

[64] J.M. Sabatier and N. Xiang. An investigation of acoustic-to-seismic coupling to detect buried antitank landmines. *IEEE Transactions on Geoscience and Remote Sensing*, 39(6):1146 – 1154, 2001.

[65] T. Sarkodie-Gyan, D. Hong, and A.W. Campbell. A novel diagnostic scheme for the classification of pistons. *Journal of Intelligent and Fuzzy Systems*, 9:101–111, 2000.

[66] V. Sequeira, G. Bostrom, M. Fiocco, D. Puig, and J. Goncalves. 3D site modelling and verification of plant design for nuclear security applications. In *Proceedings of the IEEE Conference on Computer Vision and Pattern Recognition*, pages 127 – 127, San Diego, CA, June 2005.

[67] G. Sithole and G. Vosselman. Comparison of filtering algorithms. In *Proceedings of the ISPRS Working Group III/3 Workshop on 3D Reconstruction from Airborne Laserscanner and InSAR Data*, Dresden, Germany, October 2003.

[68] D.L. Snyder and A.M. Hammoud. Image recovery from data acquired with a charge-coupled-device camera. *Journal of the Optical Society of America, A*, 10(5):1014–1022, 1993.

[69] E. Sobel, J. Douglas, and G. Ettinger. 3D LADAR ATR based on recognition by parts. In *Proceedings SPIE*, volume 5094, pages 29–40, September 2003.

[70] U. Söderman, S. Ahlberg, Å. Persson, and M. Elmqvist. Towards rapid 3d modelling of urban terrains. In *Proceedings of the Second Swedish-American Workshop on Modeling and Simulation SAWMAS-2004*, pages 184–189, Cocoa Beach, FL, USA, February 2004.

[71] U. Söderman, S. Ahlberg, M. Walldén, and T. Höglund-Kåberger. Creating high-resolution environment models for simulation and training. In *Proceedings EuroSIW 2006*, pages 06E–SIW–042, Stockholm, Sweden, 2006.

[72] H. Song, S. Lee, J. Kim, and K. Sohn. Three-dimensional sensor-based face recognition. *Applied Optics*, 44(5):677–687, 2005.

[73] A. Srivastava, M.I. Miller, and U. Grenander. *Bayesian Automated Target Recognition*, chapter 10.8, pages 869–881. Academic Press, 2000.

[74] O. Steinvall, L. Klasen, C. Grönwall, U. Söderman, S. Ahlberg, M. Elmqvist, H. Larsson, and D. Letalick. High resolution three dimensional laser imaging - new capabilities for the net centric warfare. In *Proceedings CIMI (Civil och Militär Beredskap)*, Stockholm, Sweden, May 2003.

[75] O. Steinvall, K. Koppari, and U. Karlsson. Experimental exaluation of an airborne depth-sounding lidar. *Optical Engineering*, 32(6):1307–1321, 1993.

[76] O. Steinvall, H. Olsson, G. Bolander, C. Carlsson, and D. Letalick. Gated viewing for target detection and target recognition. In *Proceedings SPIE*, volume 3707, pages 432–448, May 1999.

[77] O.K. Steinvall and T. Carlsson. Three-dimensional laser radar modeling. In *Proceedings SPIE*, volume 4377, pages 23–34, Orlando, FL, USA, September 2001.

[78] R. Stettner, H. Bailey, and R.D. Richmond. Eye-safe laser radar 3D imaging. In *Proceedings SPIE*, volume 5412, pages 111–116, September 2004.

[79] R. Stettner, H. Bailey, and S. Silverman. Large format time-of-flight focal plane detector development. In *Proccedings SPIE*, volume 5791, pages 288–292, September 2005.

[80] M.R. Stevens, C. Monnier, and M.S. Snorrason. Parameter adaption for target recognition in LADAR. In *Proceedings SPIE*, volume 5807, pages 201–211, May 2005.

[81] G. Tolt, P. Andersson, T.R. Chevalier, C.A. Grönwall, H. Larsson, and A. Wiklund. Registration and change detection techniques using 3D laser scanner data from natural environments. In *Proceedings SPIE*, volume 6396, page 63960A, October 2006.

[82] C.K. Toth, A. Barsi, and T. Lovas. Vehicle recognition from lidar data. In *Proceedings of ISPRS Working Group III/3 Workshop on 3D Reconstruction from Airborne Laserscanner and InSAR Data*, pages 162–166, Dresden, Germany, October 2003.

[83] G. Toussaint. Solving geometric problems with the rotating calipers. In *Proceedings of IEEE MELECON*, Athens, May 1983.

[84] H.M. Tulldahl, M. Andersson, and K.O. Steinvall. Experimental results of small target detection in airborne laser depth sounding. In *Proceedings Ocean Optics XV*, Providence, USA, September 2000.

[85] H.M. Tulldahl and K.O. Steinvall. Simulation of sea surface wave influence on small target detection with airborne laser depth sounding. *Applied Optics*, 42(12): 2462–2483, 2004.

[86] A. Vasile and R.M. Marino. Pose-independent automatic target detection and recognition using 3D LADAR data. In *Proceedings SPIE*, volume 5426, pages 67–83, September 2004.

[87] J.G. Verly and R.L. Delanoy. Model-based automatic target recognition (ATR) system for forwardlooking groundbased and airborne imaging laser radars (LADAR). *Proceedings of IEEE*, 84(2):126–163, 1996.

[88] T. Vögte and E. Steinle. Fusion of 3D building models derived from first and last pulse laserscanning data. *Information Fusion*, 6:275–281, 2005.

[89] D.W. Webster, E. Marcus, and D.M. Doria. Target acquisition in three-dimensional data. In *Proceedings SPIE*, volume 5094, pages 50–58, September 2003.

[90] M.R. Wellfare and K. Norris-Zachery. Characterization of articulated vehicles using ladar seekers. In *Proceedings SPIE*, volume 3065, pages 244–254, August 1997.

[91] T. Yano, T. Tsujimura, and K. Yoshida. Vehicle identification technique using active laser radar system. In *Proceedings of IEEE International Conference on Multisensor Fusion and Integration for Intelligent Systems*, pages 275 – 280, July-August 2003.

[92] Q. Zheng, S.Z. Der, and H.I. Mahmoud. Model-based target recognition in pulsed ladar imagery. *IEEE Transactions on Image Processing*, 10(4):565–572, 2001.

Part II

Publications

Paper A

Ground Target Recognition using Rectangle Estimation

Authors: Christina Grönwall, Fredrik Gustafsson, and Mille Millnert.

Accepted for publication in *IEEE Transactions on Image Processing*.

Preliminary version published as Technical Report LiTH-ISY-R-2735, Department of Electrical Engineering, Linköping University, Linköping, Sweden.

Paper B

3D Content-Based Model Matching using Geometric Features

Authors: Christina Grönwall and Fredrik Gustafsson.

Submitted to *Pattern Recognition.*

Preliminary version published as Technical Report LiTH-ISY-R-2726, Department of Electrical Engineering, Linköping University, Linköping, Sweden.

Paper C

Influence of Laser Radar Sensor Parameters on Range Measurement and Shape Fitting Uncertainties

Authors: Christina Grönwall, Ove Steinvall, Fredrik Gustafsson, and Tomas Chevalier.

Submitted to *Optical Engineering*.

Preliminary version published as Technical Report LiTH-ISY-R-2745, Department of Electrical Engineering, Linköping University, Linköping, Sweden.

Paper D

Performance Analysis of Measurement Error Regression in Direct-Detection Laser Radar Imaging

Authors: Christina Grönwall, Tomas Carlsson, and Fredrik Gustafsson.

Published in the *Proceedings IEEE Conference on Acoustics, Speech and Signal Processing*, Hong Kong, April 2003.

Paper E

Ground Target Recognition in a Query-Based Multi-Sensor Information System

Authors: Jörgen Ahlberg, Martin Folkesson, Christina Grönwall, Tobias Horney, Erland Jungert, Lena Klasén, and Morgan Ulvklo

To be submitted.

Preliminary version published as Technical Report LiTH-ISY-R-2748, Department of Electrical Engineering, Linköping University, Linköping, Sweden.

Paper F

Approaches to Object/Background Segmentation and Object Dimension Estimation

Authors: Christina Grönwall and Fredrik Gustafsson.

Technical Report LiTH-ISY-R-2746, Department of Electrical Engineering, Linköping University, Linköping, Sweden.

Notation

Symbols and Operators

$\mathbf{I}$	Identity matrix
$\mathbf{R}$	Rotation matrix
$\mathbf{T}$	Translation vector
$\mathbf{1}$	Column vector with ones, i.e., $\mathbf{1} = (1, 1, ..., 1)^t$
$\mathbf{0}$	Column vector with zeros, i.e., $\mathbf{0} = (0, 0, ..., 0)^t$
$\mathbf{n}$	Normal vector
R	Range between sensor and object
θ	Parameter vector
θ^0	True (usually unknown) parameter vector
$\hat{\theta}$	Estimated parameter vector
N	Length of the observed data set
J	Fisher information
$\mathcal{N}(\mu, \Sigma)$	Normal (Gaussian) distribution with mean value μ and covariance matrix Σ
$\mathcal{U}(a, b)$	Uniform distribution over the interval $[a, b]$
$\mathrm{P}o(x)$	Poisson distribution with mean value x
det A	Determinant of matrix A
tr A	Trace of matrix A
A^t	Transpose of matrix A
A^{-1}	Inverse of matrix A
$A_{i,j}$	Element in column i, row j of matrix A
min $f(x)$	Minimize
max $f(x)$	Maximize
Proj$(x \mid y)$	Projection of x onto y

$p(x \mid y)$	The probability density function for obtaining x given y
$E(\cdot)$	Expectation operator
$O(\cdot)$	Ordo operator
$\log_2$	The logarithm function with base 2
$\|\cdot\|_2$	Euclidean norm

Abbreviations and Acronyms

2D	Two dimensional
3D	Three dimensional
i.i.d.	independently and identically distributed
ladar	laser detection and ranging or laser radar
lidar	light detection and ranging
radar	radio detection and ranging
ATR	Automatic Target Recognition
CAD	Computer-Aided Design
CRLB	Cramér-Rao Lower bound
EM	Expectation Maximization
FIM	Fisher Information Matrix
FOI	Swedish Defence Research Agency
FPA	Focal Plane Array
GPS	Global Positioning System
GV	Gated Viewing
ICP	Iterative Closest Point
IR	Infrared
LS	Least Squares
MSE	Mean Square Error
PDF	probability density function

PhD Dissertations
Division of Automatic Control
Linköpings universitet

M. Millnert: Identification and control of systems subject to abrupt changes. Thesis No. 82, 1982. ISBN 91-7372-542-0.
A. J. M. van Overbeek: On-line structure selection for the identification of multivariable systems. Thesis No. 86, 1982. ISBN 91-7372-586-2.
B. Bengtsson: On some control problems for queues. Thesis No. 87, 1982. ISBN 91-7372-593-5.
S. Ljung: Fast algorithms for integral equations and least squares identification problems. Thesis No. 93, 1983. ISBN 91-7372-641-9.
H. Jonson: A Newton method for solving non-linear optimal control problems with general constraints. Thesis No. 104, 1983. ISBN 91-7372-718-0.
E. Trulsson: Adaptive control based on explicit criterion minimization. Thesis No. 106, 1983. ISBN 91-7372-728-8.
K. Nordström: Uncertainty, robustness and sensitivity reduction in the design of single input control systems. Thesis No. 162, 1987. ISBN 91-7870-170-8.
B. Wahlberg: On the identification and approximation of linear systems. Thesis No. 163, 1987. ISBN 91-7870-175-9.
S. Gunnarsson: Frequency domain aspects of modeling and control in adaptive systems. Thesis No. 194, 1988. ISBN 91-7870-380-8.
A. Isaksson: On system identification in one and two dimensions with signal processing applications. Thesis No. 196, 1988. ISBN 91-7870-383-2.
M. Viberg: Subspace fitting concepts in sensor array processing. Thesis No. 217, 1989. ISBN 91-7870-529-0.
K. Forsman: Constructive commutative algebra in nonlinear control theory. Thesis No. 261, 1991. ISBN 91-7870-827-3.
F. Gustafsson: Estimation of discrete parameters in linear systems. Thesis No. 271, 1992. ISBN 91-7870-876-1.
P. Nagy: Tools for knowledge-based signal processing with applications to system identification. Thesis No. 280, 1992. ISBN 91-7870-962-8.
T. Svensson: Mathematical tools and software for analysis and design of nonlinear control systems. Thesis No. 285, 1992. ISBN 91-7870-989-X.
S. Andersson: On dimension reduction in sensor array signal processing. Thesis No. 290, 1992. ISBN 91-7871-015-4.
H. Hjalmarsson: Aspects on incomplete modeling in system identification. Thesis No. 298, 1993. ISBN 91-7871-070-7.
I. Klein: Automatic synthesis of sequential control schemes. Thesis No. 305, 1993. ISBN 91-7871-090-1.
J.-E. Strömberg: A mode switching modelling philosophy. Thesis No. 353, 1994. ISBN 91-7871-430-3.
K. Wang Chen: Transformation and symbolic calculations in filtering and control. Thesis No. 361, 1994. ISBN 91-7871-467-2.
T. McKelvey: Identification of state-space models from time and frequency data. Thesis No. 380, 1995. ISBN 91-7871-531-8.
J. Sjöberg: Non-linear system identification with neural networks. Thesis No. 381, 1995. ISBN 91-7871-534-2.
R. Germundsson: Symbolic systems – theory, computation and applications. Thesis No. 389, 1995. ISBN 91-7871-578-4.
P. Pucar: Modeling and segmentation using multiple models. Thesis No. 405, 1995. ISBN 91-7871-627-6.
H. Fortell: Algebraic approaches to normal forms and zero dynamics. Thesis No. 407, 1995. ISBN 91-7871-629-2.

A. Helmersson: Methods for robust gain scheduling. Thesis No. 406, 1995. ISBN 91-7871-628-4.
P. Lindskog: Methods, algorithms and tools for system identification based on prior knowledge. Thesis No. 436, 1996. ISBN 91-7871-424-8.
J. Gunnarsson: Symbolic methods and tools for discrete event dynamic systems. Thesis No. 477, 1997. ISBN 91-7871-917-8.
M. Jirstrand: Constructive methods for inequality constraints in control. Thesis No. 527, 1998. ISBN 91-7219-187-2.
U. Forssell: Closed-loop identification: Methods, theory, and applications. Thesis No. 566, 1999. ISBN 91-7219-432-4.
A. Stenman: Model on demand: Algorithms, analysis and applications. Thesis No. 571, 1999. ISBN 91-7219-450-2.
N. Bergman: Recursive Bayesian estimation: Navigation and tracking applications. Thesis No. 579, 1999. ISBN 91-7219-473-1.
K. Edström: Switched bond graphs: Simulation and analysis. Thesis No. 586, 1999. ISBN 91-7219-493-6.
M. Larsson: Behavioral and structural model based approaches to discrete diagnosis. Thesis No. 608, 1999. ISBN 91-7219-615-5.
F. Gunnarsson: Power control in cellular radio systems: Analysis, design and estimation. Thesis No. 623, 2000. ISBN 91-7219-689-0.
V. Einarsson: Model checking methods for mode switching systems. Thesis No. 652, 2000. ISBN 91-7219-836-2.
M. Norrlöf: Iterative learning control: Analysis, design, and experiments. Thesis No. 653, 2000. ISBN 91-7219-837-0.
F. Tjärnström: Variance expressions and model reduction in system identification. Thesis No. 730, 2002. ISBN 91-7373-253-2.
J. Löfberg: Minimax approaches to robust model predictive control. Thesis No. 812, 2003. ISBN 91-7373-622-8.
J. Roll: Local and piecewise affine approaches to system identification. Thesis No. 802, 2003. ISBN 91-7373-608-2.
J. Elbornsson: Analysis, estimation and compensation of mismatch effects in A/D converters. Thesis No. 811, 2003. ISBN 91-7373-621-X.
O. Härkegård: Backstepping and control allocation with applications to flight control. Thesis No. 820, 2003. ISBN 91-7373-647-3.
R. Wallin: Optimization algorithms for system analysis and identification. Thesis No. 919, 2004. ISBN 91-85297-19-4.
D. Lindgren: Projection methods for classification and identification. Thesis No. 915, 2005. ISBN 91-85297-06-2.
R. Karlsson: Particle Filtering for Positioning and Tracking Applications. Thesis No. 924, 2005. ISBN 91-85297-34-8.
J. Jansson: Collision Avoidance Theory with Applications to Automotive Collision Mitigation. Thesis No. 950, 2005. ISBN 91-85299-45-6.
E. Geijer Lundin: Uplink Load in CDMA Cellular Radio Systems. Thesis No. 977, 2005. ISBN 91-85457-49-3.
M. Enqvist: Linear Models of Nonlinear Systems. Thesis No. 985, 2005. ISBN 91-85457-64-7.
T. B. Schön: Estimation of Nonlinear Dynamic Systems — Theory and Applications. Thesis No. 998, 2006. ISBN 91-85497-03-7.
I. Lind: Regressor and Structure Selection — Uses of ANOVA in System Identification. Thesis No. 1012, 2006. ISBN 91-85523-98-4.
J. Gillberg: Frequency Domain Identification of Continuous-Time Systems Reconstruction and Robustness. Thesis No. 1031, 2006. ISBN 91-85523-34-8.
M. Gerdin: Identification and Estimation for Models Described by Differential-Algebraic Equations. Thesis No. 1046, 2006. ISBN 91-85643-87-4.